nature reviews chemistry

https://doi.org/10.1038/s41570-025-00765-9

Review article

Check for updates

Production of bio-based lactones as monomers for a circular polymer economy

Daniyal Kiani[1,2], Ross Eaglesfield[1,2], James H. May[1,2], Allison Z. Werner[1,2], Eugene Y.-X. Chen[3], Yuriy Román-Leshkov[4], Yomaira J. Pagán-Torres[5] & Gregg T. Beckham[1,2]

Abstract

To create a circular plastics economy, new polymers are being developed that can be chemically recycled. Circular polyesters are of particular interest and to this end, lactones are ideal monomers. This Review examines catalytic routes to convert diols, hydroxy acids, and dicarboxylic acids to lactones, focusing on the development of scalable, atom-economic, and energy-efficient conversions of bio-derived feedstocks. Free energy analysis is used to inform process choices, such as reactor type, reaction phase, and use of solvent. Catalyst design principles are summarized for both direct (bio-substrate to lactone) and indirect (bio-substrate to intermediate to lactone) routes. Finally, we summarize literature that shows that many lactone precursors are readily accessible from various metabolic and chemo-catalytic pathways. Transitioning to bio-based monomers offers an opportunity to reduce reliance on fossil carbon resources, but requires advanced catalytic processes informed by mechanistic insights.

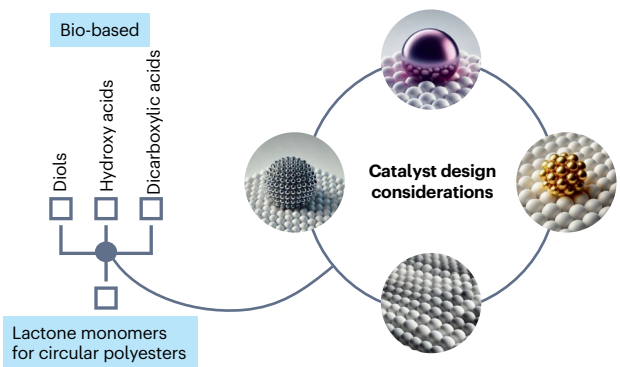

Sections

[1]Renewable Resources and Enabling Sciences Center, National Renewable Energy Laboratory, Golden, CO, USA. [2]BOTTLE Consortium, Golden, CO, USA. [3]Department of Chemistry, Colorado State University, Fort Collins, CO, USA. [4]Department of Chemical Engineering, Massachusetts Institute of Technology, Cambridge, MA, USA. [5]Department of Chemical Engineering, University of Puerto Rico — Mayagüez, Mayagüez, Puerto Rico, USA.
e-mail: gregg.beckham@nrel.gov

Introduction

It is now well recognized that the linear plastics economy exhibits negative environmental impacts driven by the continued use of fossil carbon-derived feedstocks and the lack of comprehensive end-of-life recycling solutions[1]. Addressing the plastics waste problem requires a dual strategy: transitioning to more sustainable feedstocks, such as biomass-derived building blocks or waste carbon, and incorporating circularity into polymer design[1]. A common approach in circular polymer design efforts is to incorporate a polarized, labile C–X bond (X = O, N and so on)[2–9] into the polymer backbone, enabling facile chemical depolymerization to monomers and facilitating closed-loop recycling[3,5,10–12]. In this regard, synthetic polyesters are especially prominent in the portfolio of emerging circular polymers, because they can be both bio-based, taking advantage of the inherent oxygen content in many biogenic feedstocks, and are able to be depolymerized through multiple chemical approaches[3,13].

Although many reports on circular polymers prioritize material properties and recyclability, the deployment of these polymers at scale also demands economically viable, low-emission synthesis routes for their monomers[14]. For circular polyesters, ring-opening polymerization (ROP) of both lactones and diolides (lactone dimers) provides an atom-efficient and energy-efficient route to polymer formation[2,3,9,10,15–18]. Besides ROP synthesis of polyesters, lactones find ample use in flavours and fragrance industry, as solvents, pharmaceutical agents, and so on, and thus are industrially produced at scale via energy-intensive and emissions-intensive processes, including caprolactone and valerolactone production via Baeyer–Villiger oxidation of cyclohexanone and cyclopentanone with peracetic acid[19], γ-butyrolactone production via endothermic dehydrogenation of maleic anhydride-derived 1,4-butanediol or via maleic anhydride hydrogenation[20], and β-butyrolactone production via combination of an aldehyde with a ketene[21], hydrogenation of a diketene[22], or by carbonylation of propylene epoxide[23]. These processes share two key limitations: (i) they are entirely fossil-reliant and often multistep and (ii) they are not generalizable platforms, that is, the process that yields 4-membered β-lactones is very different from the one that yields 5-membered lactones, which in turn is unique from the process for 6-membered or 7-membered lactones.

Towards a unified and bio-based approach to lactone synthesis, in this Review, we analyse chemo-catalytic pathways that can directly and indirectly convert bio-derived substrates focusing on amply available diols, hydroxy acids, and dicarboxylic acids to the corresponding lactones. We identify key challenges and opportunities for bio-based lactone monomer synthesis for circular polyesters, as illustrated in Fig. 1. This envisioned platform targets conversion of renewable carbon feedstocks[24] via biological, chemo-catalytic, or hybrid pathways[25], with maximum atom efficiency and minimal reaction steps. Our analysis first focuses on literature reports with product yields >80 mol%, especially those utilizing heterogeneous catalysts, noting their relevance to sustainable industrial processes, ease of recovery, and promise for facile scale-up. When pathways that use heterogeneous catalysts are lacking, for example, for the production of 4-membered β-lactones, we also review homogeneous catalysis studies to glean insights for effective catalyst design strategies. Specifically, we analyse the following chemo-catalytic pathways that can produce β-lactones, γ-lactones, δ-lactones, and ε-lactones:

(i) vicinal diols → epoxides → β-lactones, via carbonylation chemistry, constituting the indirect route. As carbonylation chemistry is well established[16,26–28], it is only briefly reviewed herein.
(ii) non-vicinal diols → γ-lactones, δ-lactones, ε-lactones via dehydrocyclization, through oxidative and non-oxidative pathways, constituting a direct route.
(iii) hydroxy acids → γ-lactones, δ-lactones, ε-lactones, via intramolecular esterification, constituting a direct route.
(iv) dicarboxylic acids → γ-lactones, δ-lactones, ε-lactones, via hydrogenation and intramolecular esterification, constituting a direct route.

In the last part of this Review, we review biological routes to produce diols, hydroxy acids, and dicarboxylic acids from renewable carbon feedstocks. We identify and summarize the highest reported production strains from the literature in terms of titres (overall product concentration in g l^{-1}), rates (speed of product production in g l^{-1} h^{-1}), and yields (total product as a ratio to input substrate in g g^{-1}) and report production scales where available. Most discussed pathways utilize engineered bacteria or yeast that convert carbon from either glycolysis or the tricarboxylic acid (TCA) cycle to the desired product. This pathway has the benefit of allowing cells to utilize abundant building blocks such as pyruvate or acetyl-coenzyme A (CoA) for the bioproduction of the desired molecule. Although some carbon is diverted for growth maintenance, many of these pathways achieve product yields of >30 mol% (refs. 29–32). Further genetic engineering to improve the theoretical carbon yield and minimizing flux through undesirable pathways could render these strains suitable for industrial lactone production.

Thermodynamic and reaction engineering considerations

Thermodynamics governs the feasibility and extent of chemical reactions and is essential for calculating the amount of heat exchanged during reaction. The Gibbs free energy of reaction was computed and summarized for each pathway for bio-derived epoxides and lactones in Fig. 2. In Fig. 2a, Gibbs free energy of reaction (ΔG_{rxn}) values for converting vicinal diols into epoxides indicates that the forward reaction is thermodynamically more favourable using longer-chain diols and those bearing alkyl substituents than shorter, unsubstituted analogues. Subsequent carbonylation of epoxides to β-lactones is well established and not considered in this thermodynamic analysis.

Figure 2b compares ΔG_{rxn} values for direct lactone formation from non-vicinal diols, hydroxy acids, and dicarboxylic acids. 4-Membered β-lactone formation exhibits the highest ΔG_{rxn} from all substrates owing to the high ring strain compared with larger γ-lactones, δ-lactones, and ε-lactones. Oxidative dehydrocyclization of diols to lactones produces water, a thermodynamically favourable co-product, rendering the overall reaction exergonic across lactone ring sizes. Conversely, the non-oxidative pathway co-produces hydrogen and is endergonic to varying extents depending on the lactone size. Hydroxy acids, which may be formed via hydrogenation of dicarboxylic acids, can self-esterify to form lactones and water, but these routes are also generally endergonic to varying extents, depending on the substrate chain length and the resulting lactone size.

Taken together, Fig. 2 shows that most pathways for producing epoxides and lactones from aliphatic substrates are thermodynamically uphill ($\Delta G_{rxn} \geq 0$) at standard conditions. Therefore, successfully devising a catalytic platform to produce ring-strained monomers requires concurrent research efforts on catalyst design to mitigate kinetic hindrances and reaction and reactor engineering strategies to suppress the reverse reaction through continuous separation and

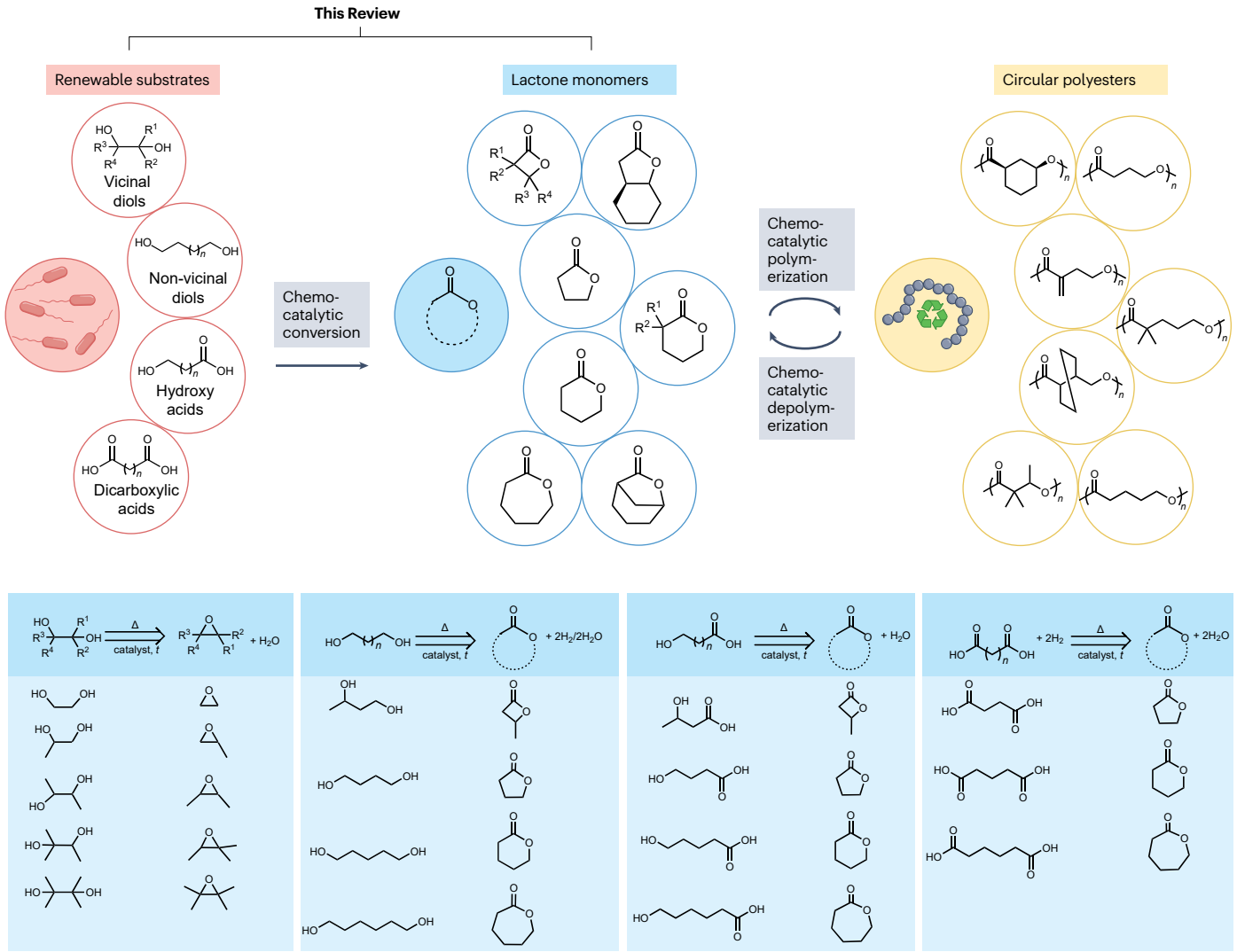

Fig. 1 | Proposed bio-derived platform to chemo-catalytically produce β-lactones, γ-lactones, δ-lactones, and ε-lactones. Monomers from diols (vicinal and non-vicinal), hydroxy acids, and dicarboxylic acids to enable circular polyesters. Balanced equations for each pathway are shown in the bottom panels.

removal of the co-products such as H_2 or H_2O to drive the forward reaction in such thermodynamically hindered pathways.

Reaction engineering considerations for efficient production of bio-based lactones need to account for the thermodynamic requirements of the reactions. Intrinsic properties of various bio-substrates such as the ΔH_{vap}, boiling point, viscosity, and so on will also be critical factors affecting the mode of reaction. To demonstrate the point, we summarize the boiling points of various terminal and vicinal diols, as well as their ΔH_{vap} values in Fig. 2c,d, which indicates that as the carbon number increases, the ΔH_{vap}, boiling point, and viscosity of the diol increase, where the viscosity is related to the ΔH_{vap} through the Eyring equation[33].

The choice between liquid-phase (semi-batch or batch process) or vapour-phase (continuous flow) operation will depend on the thermodynamic requirements of each pathway. Shorter chain diols, hydroxy acids, and dicarboxylic acids with boiling points in the range of 200–300 °C can, in principle, be reacted in the vapour phase. Literature examples of vapour-phase diol conversion to lactones report operating temperatures of 350–400 °C, especially for non-redox routes, to satisfy both thermodynamic (enthalpy of vaporization + enthalpy of reaction) and kinetic (activation energy) constraints[20,34]. When redox routes are used, lower reaction temperatures can be used, but active heat management strategies are still required to prevent runaway reactions. Even in these cases, kinetic hindrances need to be addressed with robust catalyst design strategies to lower kinetic barriers. Typically, the liquid-phase, redox dehydrocyclization of diols to lactones with the co-production of H_2O can be conducted at <200 °C in the presence of solvents[35,36].

Catalyst design considerations

Lactone production pathways can be categorized into indirect and direct routes. Indirect routes involve chemo-catalytic conversion of a bio-based substrate to an intermediate, which can then be converted to a lactone through a second, independent step – namely,

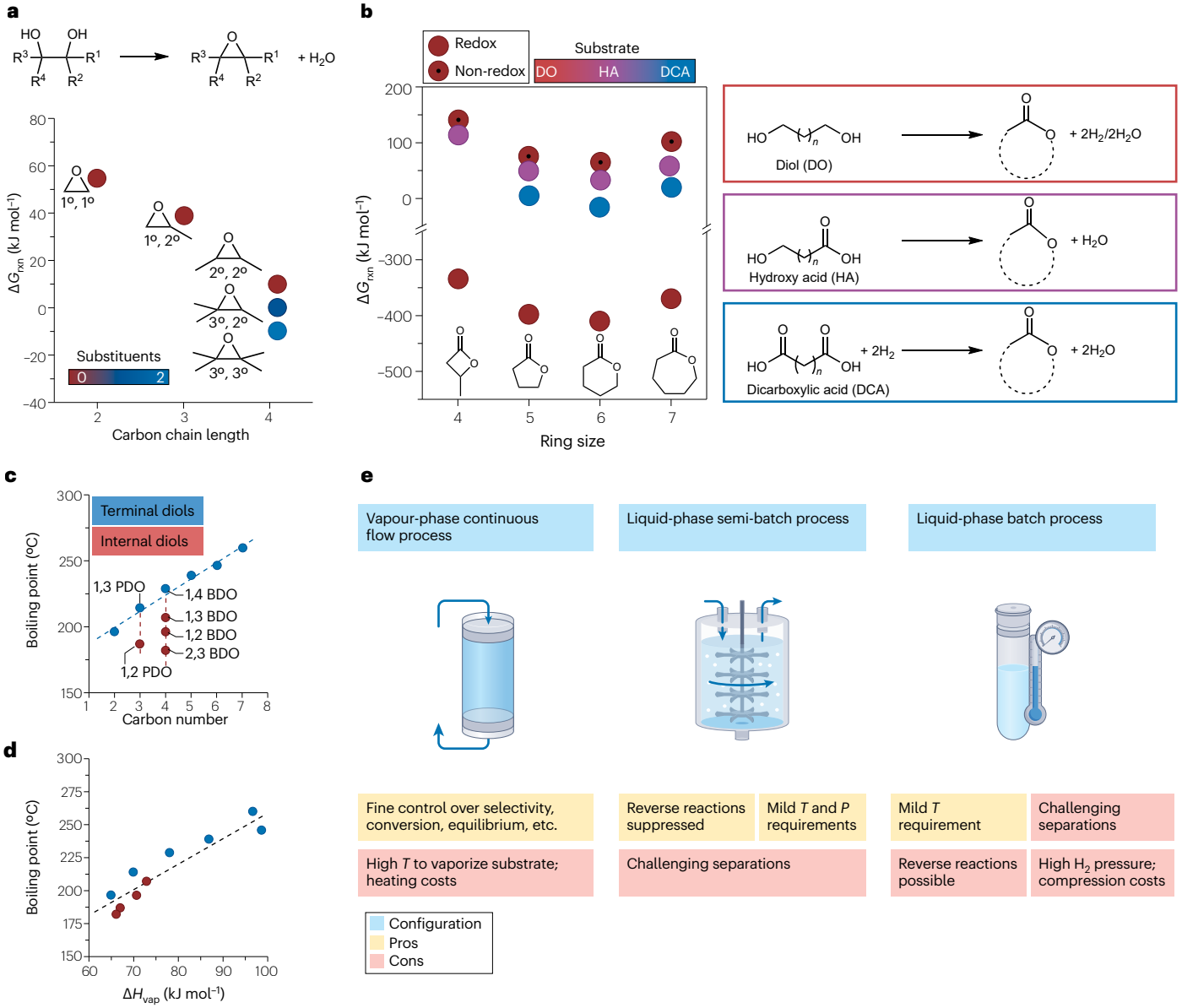

Fig. 2 | Free energy analysis of monomer production pathways and process design considerations. a, Computed Gibbs free energy of reaction at standard conditions (1 atm, 25 °C) for epoxides. The reactive carbons are labelled to highlight the degree of substitution as 1° for primary, 2° for secondary, and 3° for tertiary carbon atoms. **b**, Computed Gibbs free energy of reaction at standard conditions (1 atm, 25 °C) for lactones from bio-derived diols, hydroxy acids, and dicarboxylic acids. ΔG_{form} values are provided in the Supplementary information. **c**, Boiling points as a function of carbon number of various terminal and internal diols. **d**, Boiling points as a function of ΔH_{vap} values for various terminal and internal diols shown in part **a**. **e**, Process configurations possible for the conversion of diols, hydroxy acids, and dicarboxylic acids to corresponding lactones: continuous flow process (reactants and products flow in and out continuously), semi-batch process (reactant(s) or product(s) may flow in or out during reaction), and batch (reactants and products do not flow in or out during reaction). The semi-batch process depicted herein is rarely reported in the literature but may be suitable as a compromise between continuous flow and batch processes. BDO, butanediol; PDO, propanediol.

one catalytic cycle cannot yield the lactone product. Conversely, direct routes proceed via a single catalytic cycle, which converts bio-based substrates to the lactones without isolation and separation of an intermediate. The catalyst design considerations for indirect and direct routes for chemo-catalytic lactone production are summarized subsequently.

Indirect route

Vicinal diols to epoxides to lactones. We first review and discuss catalyst design considerations for the production of epoxide substrates. Our analysis focuses on the catalytic transformation of C_2–C_4 vicinal diols, prioritizing studies that report product yields above 80 mol%. These reactions yield strained epoxides, which serve as precursors to

β-lactones via carbonylation. The corresponding references have been summarized in Supplementary Table 1.

The catalytic conversion of vicinal diols to their corresponding ring-strained epoxides proceeds via a dehydrative elimination reaction mechanism, distinct from E_1 or E_2 acid-catalysed mechanisms[37]. The accepted pathway is a base-catalysed S_{N2}-type substitution, with the forward rate increasing as the degree of substitution increases on the oxygen-bound carbon atoms of the vicinal diol[38]. This is consistent with the Thorpe–Ingold effect, whereby increased substitution favours intramolecular cyclization[39].

To understand catalyst design principles for this reaction, we analysed the most often reported catalyst formulations for dehydrative epoxidation of vicinal diols to epoxides (Fig. 3a,b). Our analysis indicates that most catalysts are composed of alkali and alkaline-earth oxides, hydroxides, and bi(carbonates), notably Na^+, K^+, and especially Cs^+, supported on weakly acidic supports such as SiO_2. We note that although most of the literature focuses on ethylene oxide synthesis, highly substituted epoxides (for example, 2,3-dimethylbutene oxide) would yield lactones that are more useful as monomers for recyclable polyesters[15,40]. Limited examples of

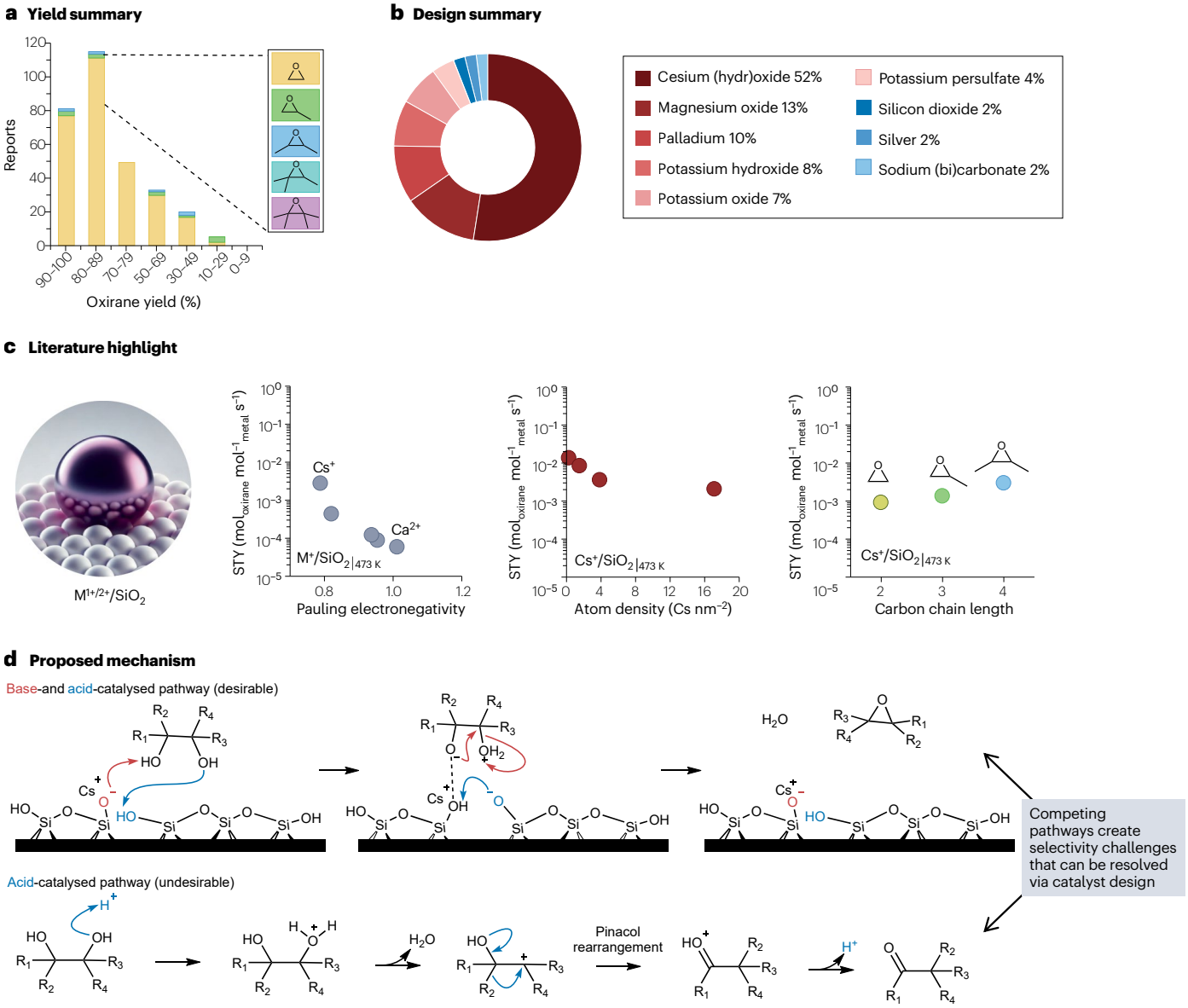

Fig. 3 | Conversion of diols to epoxides. a, Summary of bibliometric analysis on epoxide production to identify high-yield (>80 mol%) reports. **b**, Catalyst design summary of the most-reported catalyst compositions in the high-yield literature for diol conversion to epoxides. **c**, Representative literature highlights showcasing supported basic oxide catalysts, for example, Cs^+/SiO_2, for the vapour-phase conversion of diols to the corresponding epoxides as a function of catalyst formulation, surface-site density, and substrate chain length. **d**, Literature proposed surface reaction steps over Cs^+/SiO_2 catalysts for epoxide formation from vicinal diols. Literature analysis was conducted using the CAS SciFinder database for epoxide production from ethylene glycol to ethylene oxide, 1,2-propanediol to propylene oxide, 2,3-butanediol to butene oxide, and 2,3-dimethyl-2,3-butanediol to 2,3-dimethylbutene oxide. Bibliometric analysis data in parts **a** and **b** are provided in the Supplementary information. STYs, site time yields.

the use of supported transition metal or metal oxides such as Ag and Pd are also available, especially related to ethylene epoxide production from ethylene glycol. However, the active site identity remains unclear owing to limited in situ characterization. Indeed, surface sites in AgO_x and PdO_x are known to be basic and redox-active, complicating mechanistic interpretation[41].

On the basis of the frequency of reports on catalysts containing group I and II oxides and hydroxides, especially supported caesium oxide catalysts, it can be inferred that basic surface sites of optimal strength are essential for the dehydrative epoxidation mechanism. Although studies with direct mechanistic evidence are rare, several catalyst design insights emerge from the literature on the topic, exemplified in the case study shown in Fig. 3c,d. A key design parameter is the balance between surface basicity and the electronegativity of the cation. Weakly electronegative group I cations such as Cs^+ yield higher catalytic activity than K^+ and Na^+. Group II cations also form active catalysts, but exhibit site time yields (STYs) ~2 orders of magnitude lower owing to their higher cation electronegativity. Plotting the nominal STY against Pauling electronegativity shows a monotonic decrease in STY as the electronegativity increases from 0.7 to 1.3. Cations with electronegativity higher than this cut-off value (for example, Mg^{2+}) make poorly active catalysts. Finally, it is not fully understood whether the basic cation itself serves as an active site or whether its primary role is to modify support interactions and generate interfacial oxygen sites ($M^{2+/1+}$–O–support). On the basis of the proposals in literature[38,42], it appears that the oxygen atoms of the interfacial sites ($M^{2+/1+}$–O–support) are implicated in the reaction, meaning not only the supported cation's electronegativity but also that of the support's cation (for example, Si^{4+}, Al^{3+} and Ti^{4+}) likely influence activity of the interfacial O atom. This support effect has yet to be systematically studied in dehydrative epoxidation, but is conceptually related to ligand effects in surface catalysis[43–45].

An effective catalyst for dehydrative epoxidation requires a bifunctional surface comprising both Brønsted acidic protons (surface hydroxyl sites of the catalyst support) and basic sites ($M^{1+/2+}$ cations or $M^{1+/2+}$–O–Si interfacial sites). Acidic protons are necessary for concerted H_2O elimination, whereas the basic sites are involved in the intramolecular cyclization to form the epoxide[38,42]. This implies that if the acidic sites are fully titrated, for example, by depositing a monolayer of group I or II oxides, the resulting material becomes catalytically inactive for epoxide formation. The plot of STY as a function of Cs^+ surface density in Fig. 3c confirms this, where low Cs^+ coverage (~0.24 Cs_{atoms} nm^{-2}) results in STY ~1 order of magnitude higher than catalysts with high Cs^+ loading (~17 Cs_{atoms} nm^{-2})[38]. However, as the surface density of the Cs^+ increases, the nature of the Cs sites may change; at low loadings, strongly interacting sites such as Cs^+–O–Si may form, whereas at higher Cs loadings, a Cs_2O crystalline phase may form and the interaction with the catalyst support may be reduced. Mechanistic studies (Fig. 3d) further confirm that purely acidic catalysts promote elimination pathways (E1 or E2), yielding aldehydes and ketones rather than substitution products[38,46,47]. By contrast, bifunctional catalysts, such as low-loading Cs^+/SiO_2, which maintain a mixture of basic and acidic surface sites of optimal strength and in optimal proximity of each other, selectively dehydrate the vicinal diols to epoxides via a substitution pathway. Therefore, studies with quantitative site-counting methods (redox, basic, and acidic) as a function of group I or II metal oxide surface density are required to support the claim that both acidic and basic sites are necessary for the conversion to vicinal diols to epoxides. Moreover, a clear opportunity is present for rational design and compositional tuning of catalysts that promote the bifunctional pathway to steer product selectivity towards epoxides.

In terms of substrate identity, longer-chain diols such as 2,3-butanediol exhibit higher STYs than shorter chain diols such as ethylene glycol for conversion to corresponding epoxides: butene oxide > propylene oxide > ethylene oxide. Although the STY difference is less than one order of magnitude, the trend is consistent and may be due to stronger adsorption energetics of the longer chain substrates, higher stability of the reactive intermediate in more substituted carbon atoms, and the Thorpe–Ingold effect[39,48].

Finally, a sufficiently large ionic radius of the basic cations is needed to prevent their dissolution and diffusion into the lattice of the support (Li^+ and Na^+ especially do not satisfy this criterion)[49–51]. Elsewhere in the literature, it is known that smaller, group I cations such as Li^+ and Na^+ migrate into the bulk of the support, for example, SiO_2, and catalyse the transformation of amorphous SiO_2 into crystalline cristobalite phase at ~750 °C, which is well below the phase transition temperature of ~1,500 °C in the absence of these ions[50–53]. However, the exact ionic radius necessary to prevent solid solution formation is also dependent on the catalyst support utilized and the calcination temperature used. To our knowledge, stability tests to monitor the evolution of active and selective catalysts during vicinal diol conversion to epoxides have not been conducted on industrially relevant timescales. Typically, time-on-stream data for vapour-phase diol conversion in the literature is on the order of 24–96 h, and significant deactivation of catalysts is observed in these timeframes[38,42]. Although the deactivation mechanism has not been studied for such catalysts, it has been speculated that alkali leaching may be responsible for the observed deactivation[38,42]. Alternatively, carbon deposition or coke formation can also lead to catalyst deactivation as both basic and acidic surface sites can initiate coke formation.

Once an epoxide is formed, the ring-expansion carbonylation of epoxide to the corresponding lactone can be carried out over heterogenized bimetallic catalysts of the general form [Lewis acid]$^+$[$Co(CO)_4$]$^-$ (refs. 54–56). Although these heterogeneous systems have not yet matched the substrate scope or activity of their homogeneous counterparts, they represent a promising direction for developing scalable, carbonylation-based routes to lactones[28,54–56]. Additional insights into catalyst design for this step are discussed in the subsequent section on homogeneous catalysis.

Direct routes

Dehydrocyclization of non-vicinal diols. Next, we analysed the heterogeneous catalysis literature for the conversion of diols to lactones, with an emphasis on reports with high lactone yields (>80 mol%). The references are provided in Supplementary Table 2, and the most-reported catalyst components are summarized in Fig. 4a,b. Notably, the literature on β-lactones is sparse. In general, significant opportunities exist to improve this field through rigorous product analysis and quantification, catalyst performance comparisons on a per active site basis, and elucidation of the underlying surface mechanisms employing operando characterization techniques. The absence of such rigorous studies limits the ability to comprehensively derive fundamental catalyst design principles and hinders the translation of these reactions to scalable processes for ring-strained lactone production from bio-derived substrates.

As shown in Fig. 4a,b, catalysts for diol dehydrocyclization commonly contain Cu, Pt, Pd, or Au supported on basic or redox-active

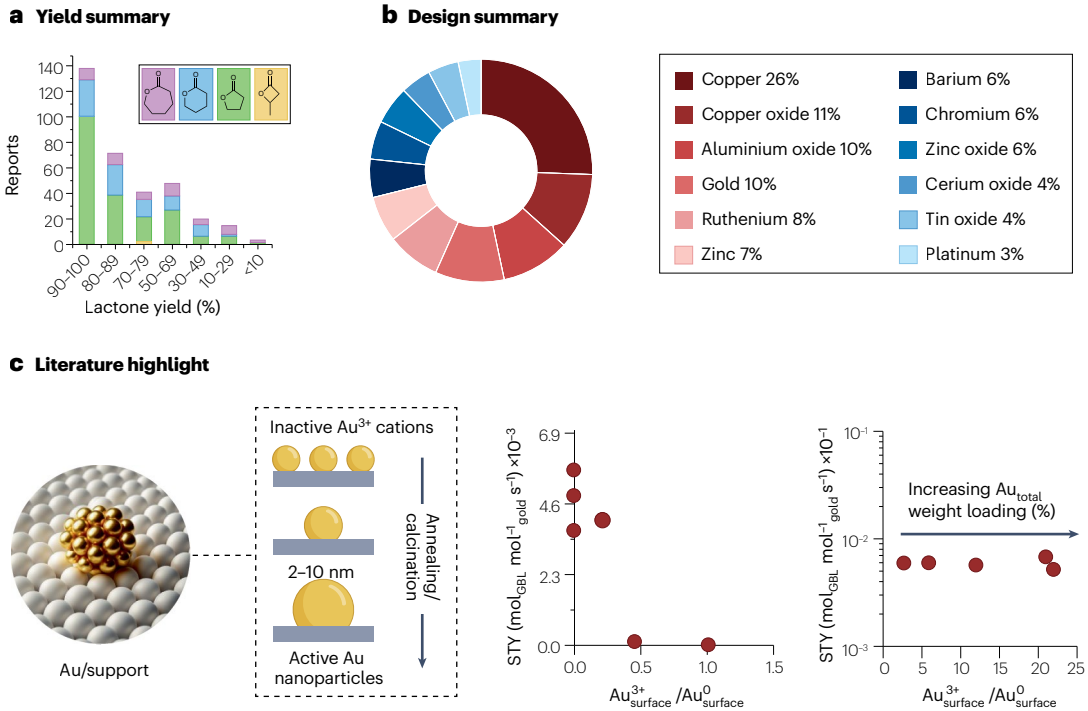

Fig. 4 | Lactone production from diols. a, Summary of bibliometric analysis on lactone production from diols to identify high-yield (>80 mol%) reports. **b**, Catalyst design summary of the most-reported catalyst compositions in the high-yield literature for diol conversion to lactones (oxidative and non-oxidative routes). **c**, Representative literature highlight showcases supported Au/TiO_2-supported catalysts for liquid-phase dehydrocyclization of various terminal diols to respective lactones, with ex situ ultrahigh vacuum X-ray photoelectron spectroscopy-based insights correlating surface Au^0 content and site time yield (STY). The representative data in panel **c** highlight the relevance of metallic Au nanoparticles for dehydrocyclization of diols[61]. Literature analysis was conducted using the CAS SciFinder database for β-lactones, γ-lactones, δ-lactones, and ε-lactones production from 3–6 membered diols. Bibliometric analysis data in panels **a** and **b** are provided in the Supplementary information.

oxides, including TiO_2, BaO, SnO_2 (ref. 35), and ZnO. The conversion of a diol to the corresponding lactone involves two dehydrogenation steps, which may occur oxidatively or non-oxidatively. Accordingly, catalysts must promote C–H bond activation and stabilize dehydrogenated intermediates, functions typically associated with basic and redox-active surfaces. When reduced metals such as Pt, Pd, Au, or Cu are used, the mechanistic role of the metallic versus oxidized state is not well understood. Some studies on Cu-based catalysts explicitly include a pre-reduction step, suggesting Cu^0 is the active phase[20,34,57,58], although other studies claim that Cu^{1+} is the active site[59]. We note that when a pre-reduced metallic catalyst is used, vapour-phase diol conversion to lactone proceeds via the non-redox route with the co-production of H_2 instead of H_2O. This reaction is conducted in the absence of O_2 or air and in the presence of H_2 flow to keep the metallic catalyst active[57].

Conversely, catalysts such as Pt/SnO_2 (ref. 35), Au/Al_2O_3 (ref. 60), Au/AlOOH[60], and Au/TiO_2 (ref. 61) are reported to be active and selective for liquid-phase diol conversion to lactones via the thermodynamically favourable redox route with co-production of H_2O. Typically, such catalysts are tested in high-pressure batch reactors, with diol dissolved in solvents such as tributyl phosphate, mesitylene, or hexanes with high-pressure air or O_2. The role of each catalyst component remains unresolved. Reduced metals may directly facilitate C/O–H activation by lowering dehydrogenation barriers and indirectly by promoting H-spillover to adjacent sites as metal-bound H species diffuse rapidly. They may also contribute to ring closure of dehydrogenated intermediates, as Pt^0 and Au^0 are known to promote cyclization reactions[62,63]. A third possibility would be that reduced metals such as Pt and Au are involved in O_2 activation to regenerate oxidized active sites, although no direct evidence currently supports this mechanism.

Owing to limited mechanistic studies on Pt-supported and Au-supported catalysts, it remains unclear whether the metals stay in the reduced state (M^0) throughout the reaction or undergo redox cycling ($M^0 \leftrightarrow M^{n+}$). For example, in Au/$TiO_2$ catalysts, ex situ ultrahigh vacuum X-ray photoelectron spectroscopy (Fig. 4c) showed that catalysts dried at <100 °C contained a higher population of oxidized cationic gold species (that is, Au^{3+}), whereas those calcined or annealed at >200 °C primarily contained reduced gold nanoparticles of 2–10 nm size (that is, Au^0)[61]. The catalysts with Au^{3+} were found to be inactive for the dehydrocyclization of diols to lactones, and those with Au^0 nanoparticles exhibited high activity and selectivity to lactone formation, implying that Au^0 was likely the active site with STY staying constant from ~2 wt% to 8 wt% Au loading. The structure-insensitive dehydrocyclization of diols to lactones has also been reported for Au/Al_2O_3 and Au/Fe_2O_3 catalysts, which were shown to contain Au^0 nanoparticles of varying sizes[60,64]. However, we note that these insights are based on ex situ characterization of fresh catalysts, and the morphology and nuclearity of the active Au species during reaction remain unidentified.

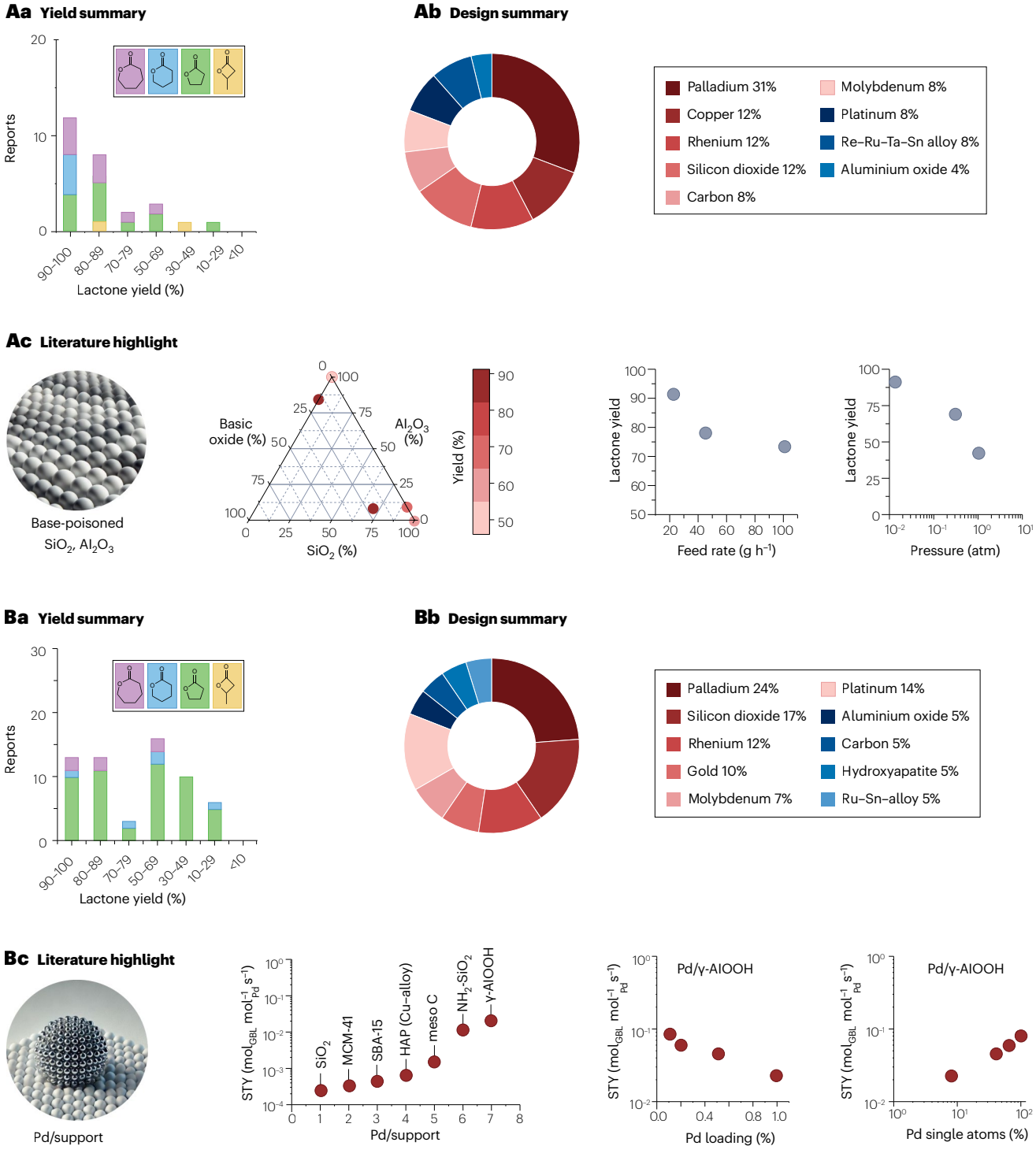

Broadly in the catalysis literature, Au/support and Cu/support catalysts have been studied for alcohol dehydrogenation reactions, where the oxidized metal sites (MO_x) are identified as the active sites as opposed to the reduced metallic sites (M^0). For example, the presence of $Cu^{\delta+}O_x$ sites on oxidic supports was shown to be necessary for an active alcohol dehydrogenation catalyst[65–67]. Likewise, $Au^{\delta+}O_x$ sites have been proposed as the active sites for ethanol dehydrogenation as well[68–70]. Finally, another potential phenomenon that can occur during the dehydrocyclization of diols to lactones is the formation of surface-oxide overlayers from strong metal–support interaction[71], when a transition metal is supported on a reducible oxide and subjected to reductive conditions similar to pre-reduction steps reported in the diol-to lactone literature[72,73]. It is not clear whether strong metal–support interaction occurs

Fig. 5 | Lactone production from hydroxy acids and diacids. Aa, Summary of bibliometric analysis on lactone production from hydroxy acids to identify high-yield (>80 mol%) reports. **Ab**, Catalyst design summary of the most-reported catalyst compositions in the high-yield literature for hydroxy acid conversion to lactones. **Ac**, Representative literature highlight showcasing bifunctional catalysts, identifying the base-poisoned acidic oxides for vapour-phase, intramolecular esterification of hydroxy acids to lactones, and the effects of catalyst composition, space velocity, and reaction pressure on the lactone yield from ref. 76. The literature analysis was conducted using the CAS SciFinder database for β-lactones, γ-lactones, δ-lactones, and ε-lactones production from 4–6 membered hydroxy acids. **Ba**, Summary of bibliometric analysis on lactone production from diacids to identify high-yield (>80 mol%) reports. **Bb**, Catalyst design summary of the most-reported catalyst compositions in the high-yield literature for dicarboxylic acid conversion to lactones. **Bc**, Representative literature highlight showcasing supported Pd catalysts, evidencing the critical role of acidic catalyst support, and small Pd morphology for creating an active catalyst for reduction and esterification of dicarboxylic acids to lactones from ref. 82. The literature analysis was conducted using the CAS SciFinder™ database for γ-lactones, δ-lactones, and ε-lactones production from 4–6-membered dicarboxylic acids. Bibliometric analysis data in parts **A** and **B** are provided in the Supplementary information.

during the reaction conditions and, if so, whether it is sufficiently significant to cause site blockage of the Au/support and Pt/support catalysts as an impermeable oxide shell forms around the metal nanoparticles.

The design principles summarized herein (transition metal supported on basic or redox-active oxide, for example, Au/TiO_2 or Pt/SnO_2, or transition metal oxide and basic oxide promoter supported on non-reducible oxide, for example, CrO_x–BaO_x/SiO_2 or CuO_x–CrO_x/ZnO) provide a useful starting point for future research. However, rational design of stable catalysts for oxidative dehydrocyclization of diols to lactones in the liquid phase will require systematic studies to determine the structure and composition of active metal oxide phases, the electronic and geometric properties of surface sites, and the impact of H_2O on catalyst stability and reactivity. Moreover, if catalyst deactivation is observed, the underpinning mechanisms need to be investigated thoroughly, as it is known in the broader literature that terminal diols such as 1,4-butanediol and 1,6-hexanediol can readily dehydrate in the liquid state on metallic catalysts (for example, Pt/support) at low temperatures to form irreversibly bound olefin species on the surface that rapidly deactivate the catalyst via fouling[74] or cause metal leaching via chelation.

Intramolecular esterification of hydroxy acids. Figure 5 summarizes the catalyst components most frequently used for the conversion of hydroxy acids to lactones, a transformation that proceeds via intramolecular esterification catalysed by solid acids[37]. As expected, acidic oxides such as Al_2O_3, SiO_2, and SiO_2-Al_2O_3 (Fig. 5Aa,b) are commonly used. The presence of Lewis acidic and oxophilic metal oxides, such as ReO_x (ref. 75), as catalyst promoters is also consistent with this dehydrative self-esterification reaction being acid-catalysed. However, similar to the literature on diol-to-lactone conversions, the role of reduced transition metals (for example, Pt, Pd, and Cu) remains ambiguous. Their presence in some studies likely reflects the inclusion of multistep transformations involving dicarboxylic acids, in which hydroxy acids serve as intermediates in route to lactones. Focusing on reports that exclusively study the conversion of hydroxy acids to lactones (instead of dicarboxylic acids to hydroxy acids to lactones), common catalysts include acidic oxides, for example, SiO_2, Al_2O_3, or a mixture thereof, often modified with low levels of basic promoters such as group I and II oxides (Fig. 5Ac). For instance, a Union Carbide patent reported nearly quantitative yields for the vapour-phase conversion of aqueous hydroxy acids (10 wt% solutions of 5-hydroxypentanoic acid and 6-hydroxyhexanoic acid) to valerolactone and caprolactone, respectively, using a mixed oxide catalyst containing 20% CaO, 72% SiO_2, and 8% Al_2O_3 (ref. 76). This vapour-phase conversion of aqueous hydroxy acids was conducted at temperatures from 250 °C to 350 °C, sub-ambient pressures of ~0.013–0.329 atm, and low space velocities. Interestingly, if ambient pressure was used while other reaction conditions were maintained, the product selectivity switched from lactones to oligomers of the hydroxy acid. Likewise, other similar catalyst compositions have also been reported for hydroxy acid intramolecular esterification to lactones over base-poisoned acidic oxides, for example, 16% CaO, 0.1% Na, and balance of γ-Al_2O_3 (ref. 76) and 62% nano-SiO_2 with 38% β-Al_2O_3 (ref. 77). In this context, β-Al_2O_3 likely refers to β-alumina, a non-stoichiometric sodium polyaluminate (general formula: $Na_{1+x}Al_{11}O_{17+x/2}$), rather than a true Al_2O_3 polymorph[78].

Reduction and esterification of dicarboxylic acids. Dicarboxylic acids cannot be directly converted to lactones given the presence of two carboxylic groups, but rather one of the carboxylic groups needs to be reduced to a hydroxy group, yielding a hydroxy acid intermediate, which can then undergo dehydrative self-esterification to form the lactone. Alternatively, both carboxylic groups can be reduced to a diol, which can then be dehydrocyclized to a lactone. In either pathway, catalytic conversion of dicarboxylic acids to lactones requires an initial reduction of the starting substrate via hydrogenation. This reaction is typically run in the liquid phase in batch reactors at high H_2 pressures (for example, 60–150 bar) in the presence of non-reducible solvents such as 1,4-dioxane or H_2O[79–83].

Figure 5Ba,b summarizes the literature and highlights that the most often supported transition metals, for example, Pt, Pd, Ru–Sn alloys[79,81,82,84], or metal carbides such as MoC[85,86] are used for this reaction. These metals and metal carbides are known to be active hydrogenation catalysts. Oxides such as SiO_2, Al_2O_3, TiO_2, and AlOOH are frequently used to disperse the metal phase and provide surface Brønsted acid sites required for the subsequent dehydrative cyclization of the hydroxy acid intermediate. The lack of basic and redox-active oxides as catalyst supports suggests that full reduction to diols does not occur under these conditions; if diols were intermediates, as discussed previously, their cyclization would require redox-active or basic supports. Notably, these supports are not poisoned with basic modifiers, in contrast to hydroxy acid cyclization catalysts. This observation may indicate that, in the presence of H_2, the esterification step proceeds via a mechanistically distinct pathway that does not require suppression of basic sites.

To illustrate some of the salient features of catalysts used for dicarboxylic acid conversion to corresponding lactones, we highlight supported Pd-based catalysts for the liquid-phase hydrogenation of succinic acid to γ-butyrolactone in Fig. 5Bc. A relative comparison of STYs indicates that AlOOH and NH_2-functionalized SiO_2 make superior catalyst supports, attributed to their ability to highly disperse

Pd species. Poorly dispersed catalysts form large Pd particles, which lowers Pd utilization. This effect is clearly demonstrated by plotting STY as a function of Pd loading and dispersion. Specifically, in Pd/AlOOH systems, increasing Pd loading from 0.1 wt% (fully dispersed) to 1 wt% (only ~10% dispersed) leads to nearly an order-of-magnitude decrease in STY[82]. Overall, the nature of the metal species, that is, particle morphology, nuclearity, oxidation state, alloy versus mono-metallic, and the balance of the metallic sites (for hydrogenation) to the surface-acid sites (for esterification), is expected to be critical for controlling catalytic activity and selectivity of heterogeneous catalysts for the liquid-phase conversion of dicarboxylic acids to lactones.

Catalyst design summary

In summary, although rational catalyst design will require further efforts to understand the role of various catalyst components, the general strategies for catalytic conversion of diols, hydroxy acids, and dicarboxylic acids to the corresponding epoxides and lactones are grounded in the mechanistic requirements of each transformation, as depicted in Fig. 6. Each substrate follows a unique reaction pathway, requiring catalytic functionalities to overcome specific kinetic barriers, as summarized subsequently:

(i) vicinal diols to epoxides: submonolayer coverages of group I basic oxides are required to promote dehydrative S_N2 epoxidation (Fig. 6a);
(ii) diols to lactones (oxidative pathway): redox-active or basic oxide catalysts are required to promote dehydrocyclization, yielding H_2O co-product (Fig. 6b);
(iii) diols to lactones (non-oxidative pathway): supported metal catalysts promote dehydrocyclization, co-producing H2 (Fig. 6b);
(iv) hydroxy acids to lactones: base-promoted acidic oxide catalysts enable intramolecular esterification via dehydration (Fig. 6c);
(v) dicarboxylic acids to lactones: acidic oxide-supported metal catalysts for tandem hydrogenation to hydroxy acids and subsequent intramolecular esterification to lactones (Fig. 6d).

Homogeneous catalysis for 4-membered β-lactones

As shown in Figs. 4–6, there is a large body of research for the synthesis of 5-membered γ-lactones, 6-membered δ-lactones, and 7-membered ε-lactones. By contrast, catalytic strategies for β-lactone synthesis are rare, particularly in the context of heterogeneous catalysis. To address this gap, we briefly discuss homogeneous catalyst systems with an emphasis on β-lactone formation.

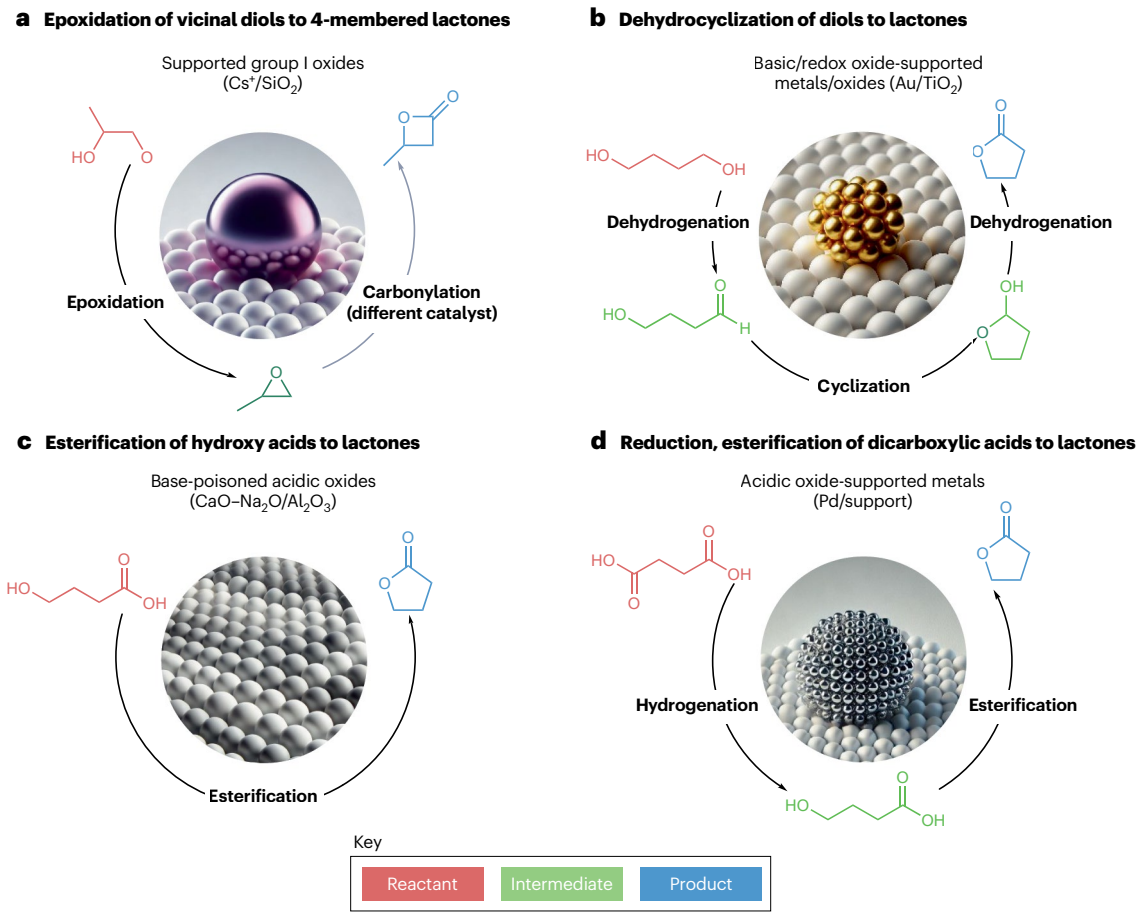

Fig. 6 | Summary of key catalytic steps in circular monomer production. **a**, Epoxidation vicinal diols followed by carbonylation to β-lactones. **b**, Dehydrocyclization of non-vicinal diols to β-lactones, γ-lactones, δ-lactones, and ε-lactones (redox and non-redox routes). **c**, Intramolecular esterification of hydroxy acids to β-lactones, γ-lactones, δ-lactones, and ε-lactones. **d**, Reduction and esterification of dicarboxylic acids conversion to γ-lactones, δ-lactones, and ε-lactones, highlighting the demands of each route that dictate catalyst design.

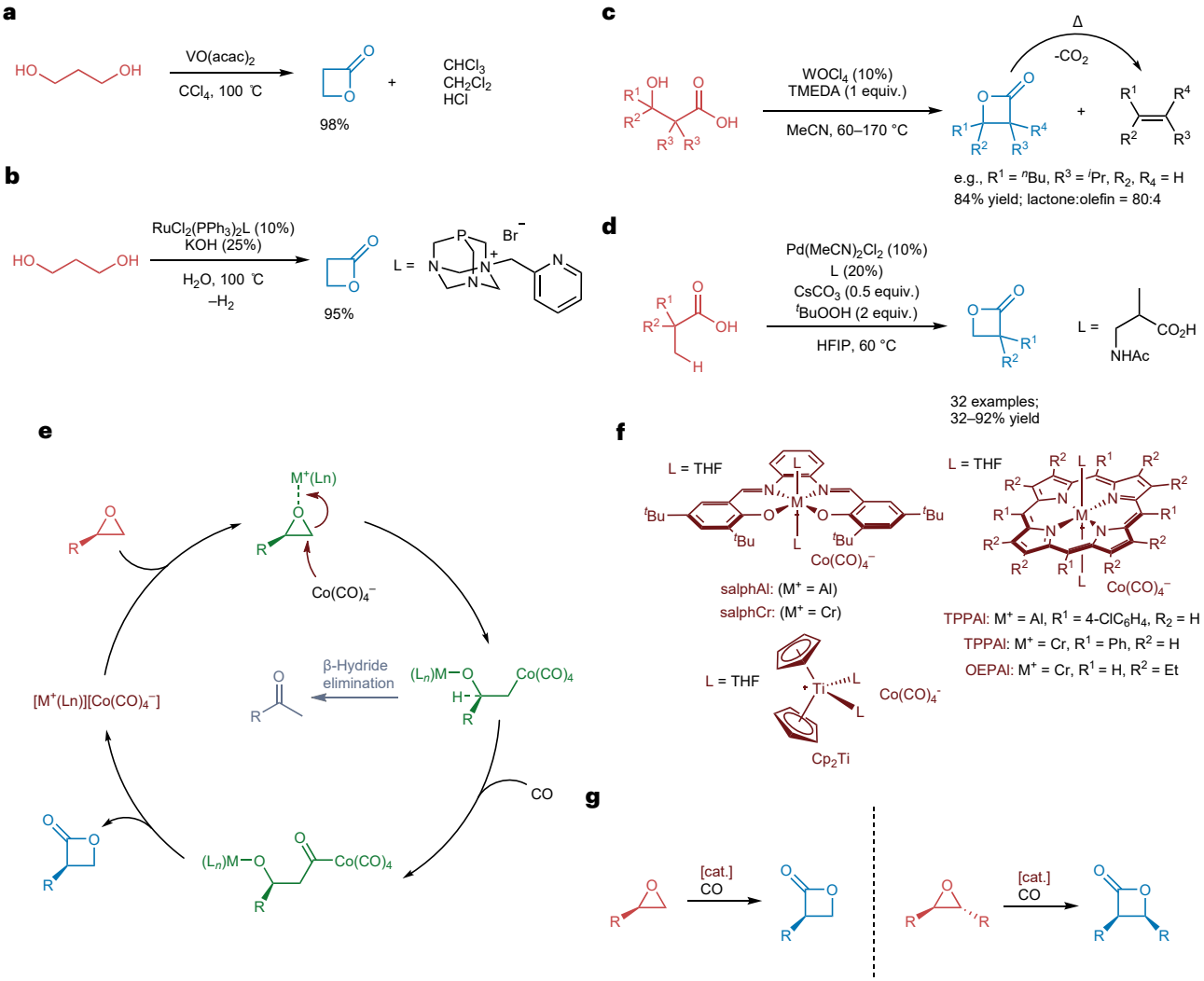

Fig. 7 | Homogeneous catalytic routes to 4-membered lactones. **a**,**b**, Homogeneously catalysed reaction for the conversion of 1,3-propanediol to propiolactone using V-catalysed and Ru-catalysed routes, respectively. **c**, $WOCl_4$-catalysed conversion of β-hydroxy acids to β-lactones. **d**, Pd-catalysed β-C(sp^3)–H functionalization of alkyl carboxylic acids to α,α-disubstituted β-lactones. **e**, Mechanism of $Co(CO)_4^-$-catalysed ring-expansion carbonylation of epoxides. **f**, Examples of highly active homogeneous catalysts for epoxide carbonylation. **g**, Regioselectivity and stereoselectivity observed in the $Co(CO)_4^-$-catalysed carbonylation of monosubstituted and 1,2-disubstituted epoxides. cat., catalyst; HFIP, hexafluoroisopropanol; TMEDA, tetramethylethylenediamine; MeCN, acetonitrile; THF, tetrahydrofuran; TPP, tetraphenylporphyrin; Salph, *N*,*N*′-bis(3,5-di-tert-butylsalicylidene)phenylenediamine; OEP, octaethylporphyrinato.

Typical synthetic procedures for preparing β-lactones rely on stoichiometric reagents that generate intermediates that spontaneously cyclize. Truly catalytic methods that directly convert bio-derived substrates (for example, 1,3-diols and β-hydroxy acids) to β-lactones are limited to a handful of examples. Only two reports were found for the direct conversion of 1,3-diols to β-lactones via homogeneous catalysts, both describing transformation of 1,3-propanediol to β-propiolactone (Fig. 7a,b). The first proceeds by action of CCl_4 in the presence of $VO(acac)_2$ catalyst, through the formation of alkyl hypochlorite intermediates[87]. Although β-propiolactone yield is high (98%), the need for CCl_4, which is sacrificial in the reaction, renders this route challenging for industrialization. A second route involves aqueous-phase oxidation of 1,3-propanediol to β-propiolactone in 95% yield using an Ru homogeneous catalyst, yielding β-propiolactone in 95% yield with H_2 as the sole by-product[88]. Although promising, this system has not been reported for other substrates to our knowledge.

Only one study reports catalytic β-lactone formation from β-hydroxy acids. In examining $WOCl_4$ as an analogue to vanadium-based catalysts for olefin production, β-lactones were observed as intermediates in two cases[89] (Fig. 7c). However, the intended transformation was olefin formation via thermal degradation of the β-lactone rather than maximizing lactone selectivity. More recently, Pd-catalysed β-C(sp^3)–H functionalization of alkyl carboxylic acids to generate various α,α-disubstituted β-lactones was also reported[90] (Fig. 7d). Despite its synthetic utility, this method requires 10 mol% Pd, a 200 mol% peroxide oxidant, and hexafluoroisopropanol as solvent, limiting its scalability. Collectively, these examples illustrate the

significant challenges associated with developing catalytic routes to β-lactones from bio-derived substrates. The limited number of examples and the absence of generalizable design principles highlight the need for further mechanistic and synthetic developments in this area.

By contrast, the indirect route involving ring-expansion carbonylation of epoxides to β-lactones is more extensively studied and mechanistically well understood[27]. The most active and selective catalysts for these transformations are bimetallic catalysts of the general form [Lewis acid]$^+$[Co(CO)$_4$]$^-$ (refs. 91,92) (Fig. 7e). The Lewis acid component is critical to activate the epoxide towards nucleophilic attack by Co(CO)$_4^-$ and stabilize the resulting intermediate. However, it must be sufficiently labile to promote facile ring closure, requiring a balance of Lewis acid strength to ensure low barriers throughout the catalytic cycle.

Catalysts developed by Coates and co-workers exemplify this approach, delivering high β-lactone yields at low catalyst loadings, low temperatures, and relatively low CO pressures[26,93–96] (Fig. 7f). The Lewis acid component in these systems typically comprises cationic salen or porphyrin complexes of Al^{3+} or Cr^{3+}, with the porphyrin complexes generally exhibiting the highest activity. The Co(CO)$_4^-$ anion serves as the nucleophile and carbonyl source.

A key advantage of this method is its ability to provide β-lactones with a high degree of regio and stereo control. For monosubstituted epoxides, Co(CO)$_4^-$ selectively adds to the unsubstituted carbon such that CO insertion occurs to produce β-substituted lactones with excellent conservation of enantiopurity (Fig. 7g). For 1,2-disubstituted epoxides, as Co(CO)$_4^-$ reacts in an S_N2 fashion, stereochemical inversion occurs at the carbon adjacent to the inserted carbonyl, such that *cis*-epoxides give *trans*-lactones and *trans*-epoxides give *cis*-lactones. Regiochemical fidelity is lost in several scenarios. Asymmetrical 1,2-disubstituted epoxides are not carbonylated with site selectivity, but yield an approximate 1:1 mixture of the two possible isomers[97]. In the case of 1,1-disubstituted epoxides – although Co(CO)$_4^-$ still displays some preference for attack at the unsubstituted carbon – the ability of the disubstituted carbon to stabilize a partial positive charge leads to a competing S_N1-type mechanism and the formation of the α,α-substituted lactone as the minor product[96]. Furthermore, in the cited review, the authors state that attempts to carbonylate trisubstituted and tetrasubstituted epoxides using Lewis acid-based catalyst were unsuccessful, resulting in mixtures of unidentified products[27]. This may limit the use of epoxide carbonylation in the production of highly substituted lactones, which have been recently shown to be valuable monomers for chemically recyclable polyhydroxyalkanoates[15].

Despite these limitations, given the high yields and atom economy, the breadth of applicable substrates, and the access to optically pure products, the ring-expansion carbonylation of epoxides is currently likely the most promising catalytic process for sustainable β-lactone production (provided the epoxides are renewable). However, difficulties associated with catalyst separation and reuse pose challenges and more work is needed to create heterogeneous catalyst analogues for these homogeneous catalysts. As previously discussed in the section on epoxide production from vicinal diols, heterogeneous catalysts for epoxide carbonylation are being developed, although their activity is lower than the activity of homogeneous counterparts. This remains an active area of research with ample opportunities in catalyst design and reaction engineering.

Biological and biomass-derived pathways to lactone precursors

Whole-cell bioconversion to the ROP-capable lactone precursors of interest from biogenic and waste carbon is a promising strategy. Bioconversion routes offer some advantages over purely chemo-catalytic routes for converting biomass-derived intermediates, most notably the ability to convert heterogeneous feedstocks to a single product in few unit operations at ambient pressure and low temperatures[98–101]. However, bioprocess metrics – such as titre (g l^{-1}), rate (g l^{-1} h^{-1}), and yield (g g^{-1}) – can be low in early research stages and require dedicated metabolic engineering and bioprocess development efforts to achieve industrial relevance. Exhaustive reviews of bioconversion pathways to the products of interest have been covered elsewhere[102–105]. Here, we highlight the state-of-the-art bioproduction systems for diol, hydroxy acid, and dicarboxylic acid lactone precursors, compare top production pathways, and discuss areas for future development. We direct interested readers to Supplementary information for a representative literature summary of biological and biomass-derived chemo-catalytic routes for C_{4-7} linear precursors including diols, hydroxy acids, and dicarboxylic acids. Cyclic-lactone precursors that may yield bicyclic lactones, for example, benzenedimethanol, cyclohexanedimethanol, and so on, remain challenging to access via whole-cell microbial routes, representing a promising avenue for future research. Biomass-derived chemo-catalytic routes to such cyclic precursors have been reported in the literature, although they are indirect and produce <80% carbon yields, and hence are not discussed in detail. Briefly, examples include isobenzofuran-1(3H)-one (also called phthalide) produced via hydrogenation of corn-stover-derived phthalic anhydride[106,107]. Alternatively, the phthalic anhydride precursor can also be produced via bio-derived furan and maleic anhydride[108]. Finally, isomers of cyclohexanedimethanol can be produced via multistep route from plant-based acrylate and acetaldehyde[109,110].

Corresponding to the aforementioned ROP-capable lactones, the most promising biological conversion pathways to C_4–C_6 diols, hydroxy acids, and dicarboxylic acids on the basis of titre were analysed with preference given to the most industrially relevant feedstocks (Supplementary Fig. 1). In total, 13 bioproducts were analysed with both vicinal and non-vicinal diols being considered. Both 1,6-hexanediol and the corresponding hydroxy acid (6-hydroxyhexanoic acid) have not been produced using whole-cell bioconversions to the best of our knowledge despite a singular patent report[111], although notably various promising biomass-derived chemo-catalytic routes have been reported. For example, cellulose-derived tetrahydrofurandimethanol hydrogenation to 1,6 hexanediol over bifunctional catalysts contains both metallic and acid sites, for example, Pt-WO_x/TiO_2 and Rh-ReO_x/SiO_2, with high selectivity (80–100%)[112,113] and 1,6-hexanediol from cellulose-based tetrahydropyran-2-methanol via tandem dehydration–hydration and hydrogenation[114]. Otherwise, all the lactone precursors have been produced in aerobic and anaerobic bacteria and fungi.

C_4 bioproducts can be produced via the central carbon intermediates pyruvate and acetyl-CoA, C_5 bioproducts predominantly via amino acid biosynthesis, and the only C_6 bioproduct reported was produced via TCA cycle intermediates (Fig. 8a and Supplementary Fig. 1). Hydroxy acids synthesis often mimics biological pathways for the corresponding diol, as diols are normally a CoA-transferase or reductive step downstream of the hydroxy acid.

Despite more complex enzymatic reactions being required to access many of the larger bioproducts, a linear trend in yield as

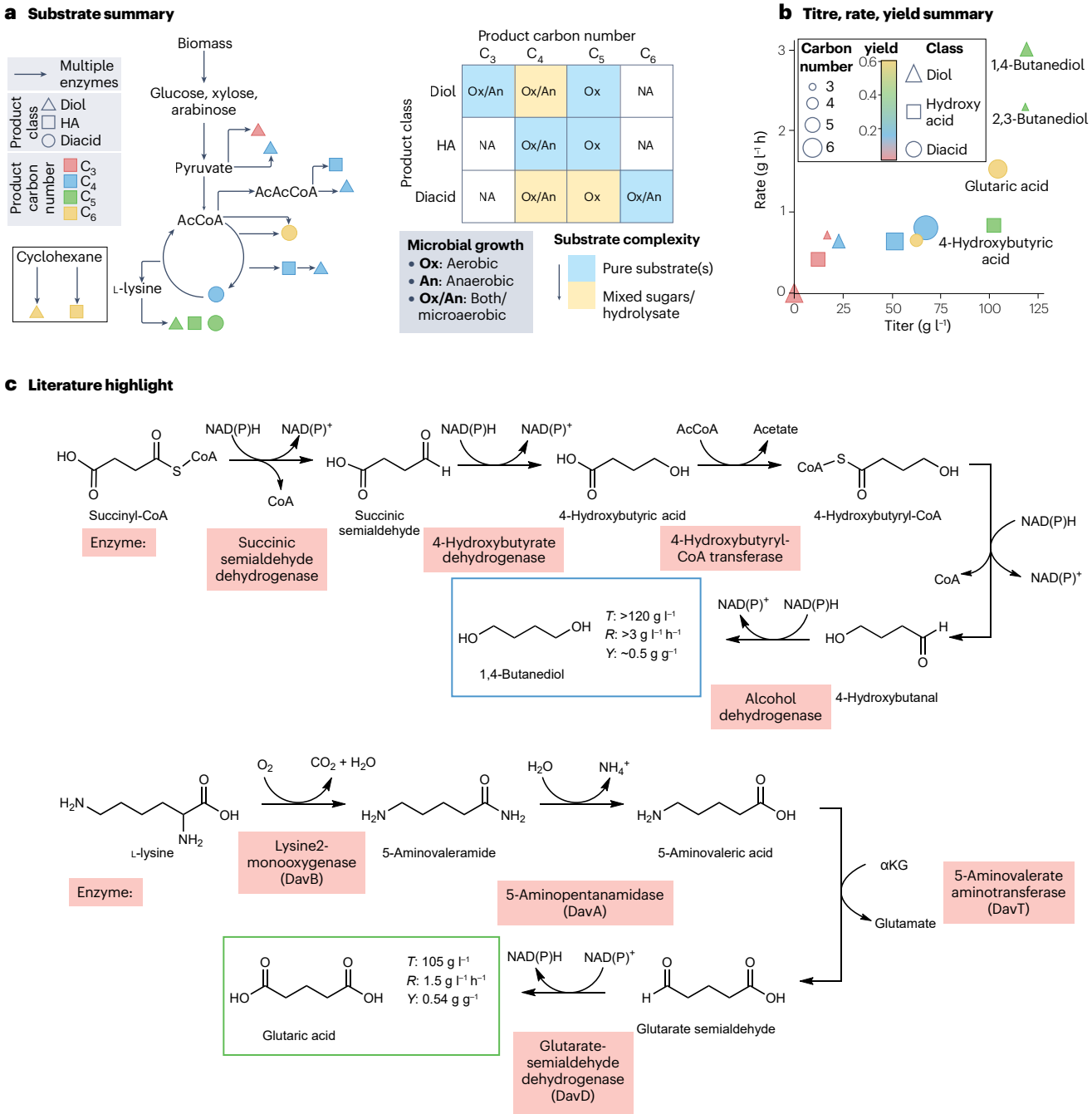

Fig. 8 | Overview of bioconversion processes to produce diols, hydroxy acids, and dicarboxylic acids. a, Simplified depiction of metabolic pathways from biomass-derived sugars to C_3–C_6 diols, hydroxy acids, and diacids. The colour of each shape represents the carbon number. A summary of the substrates used in studies producing C_3–C_6 diols, hydroxy acids, and diacids, with specific carbon sources for each product indicated in Supplementary Fig. 1. Aerobic and anaerobic cultivations are indicated by 'Ox' and 'An', respectively; while 'Ox/An' represents when both have been used or controlled microaerobic conditions were investigated. **b**, Summary of the maximum titres, rates, and yields achieved corresponding to the studies summarized in Supplementary Fig. 1. **c**, Literature highlight of 1,4-butanediol and glutaric acid bioproduction pathways. Interested readers are directed to the Supplementary information for further discussion and citation summary of various pathways to diol, hydroxy acid, and dicarboxylic acid production. DA, dicarboxylic acid; HA, hydroxy acid; NA, not available.

a function of carbon number was not observed (Supplementary Fig. 2) with yields ranging from 0.02 g g^{-1} to 0.63 g g^{-1}. Notably, the highest-reported titres analysed here correspond to a ranging complexity of substrates, from direct precursors (for example, L-lysine for 1,5-pentanediol) to corn-stover hydrolysate (Fig. 8a), indicating that there is no trend in titre as a function of substrate complexity.

Together, for these particular bioproducts, this de-emphasizes the importance of the target as predictor of success and instead points to the importance of optimal metabolic pathway design within the context of the selected microbial chassis combined with bioprocess development. For example, metabolic pathways with high NADH and NADPH demand typically require aerobic conditions, albeit oxygen saturation levels need to be carefully balanced to favour product synthesis[30,115,116], and products derived from amino acid biosynthesis are optimal in L-lysine-overproducing bacteria such as *Corynebacterium glutamicum*[30,32].

Bioprocess economic viability can be roughly approximated by a combination of the titre, rate, and yield; although no universal value exists as substrate cost, bioproduct value and other process costs vary substantially. Six of the 13 bioproducts are produced at titres exceeding 50 g l^{-1}, while simultaneously having productivities exceeding 0.66 g l^{-1} h^{-1} (Fig. 8b). 1,4-Butanediol[117] and glutaric acid[30] are highlighted as illustrative examples showing the pathways and metabolic engineering steps that were required to produce these compounds at industrially relevant quantities (Fig. 8c).

1,4-Butanediol is produced biologically at commercial scale in Europe and North America, including by Genomatica and Qore[118,119]. A computational and systems biology-informed metabolic engineering strategy developed a 5-step pathway in *Escherichia coli* from the TCA cycle intermediate succinyl-CoA through 4-hydroxybutyric acid to the non-native product, 1,4-butanediol, with acetate recycling (Fig. 8c and Supplementary Fig. 1). Design of this pathway also led to the discovery of novel enzymes for the reduction of 4-hydroxybutyryl-CoA to 1,4-butanediol using *E. coli* as a production host. The final engineered strain has been reported to produce titres of >120 g l^{-1} at close to the theoretical yield of 0.5 g g^{-1} and rates of >3 g l^{-1} h^{-1} at scale from various biomass-derived sugars[117].

Glutaric acid is not currently produced at an industrial scale biologically to our knowledge; however, reported titre, rate, and yield metrics from the literature place it in a strong position for industrial scale production in the future[30,120]. Five-carbon molecules, such as glutaric acid, are hard to produce biologically owing to the lack of C_5 precursors from central metabolism. A solution to this problem is to oxidatively decarboxylate the amino acid L-lysine using enzymes found in the *Pseudomonas* genus of bacteria. Using this strategy, a 4-step pathway was engineered in the L-lysine-overproducing bacteria *C. glutamicum*. Careful optimization of fermentation metrics such as feedstock concentration, pH, and dissolved oxygen content led to a final engineered strain reported to produce 105 g l^{-1} at an impressive yield of 0.54 g g^{-1} and a rate of 1.5 g l^{-1} h^{-1}, although at this stage only from pure glucose[30]. Finally, in terms of biomass-derived chemo-catalytic pathways to C_5 substrates, notable examples include furfural hydrogenation to 1,5-pentanediol in yields exceeding 95% over Ru/C catalysts[121,122], and δ-valerolactone production via dehydrogenation of 2-hydroxytetrahydropyran over Cu/SiO_2 (ref. 123).

Conclusions

Circular polyesters can be readily synthesized via ROP of ring-strained lactones in an atom-efficient and energy-efficient manner. In this Review, we explore catalytic routes for converting bio-based intermediates, including diols, hydroxy acids, and dicarboxylic acids to lactone monomers. Specifically, our analysis covers both direct routes (bio-substrate → lactone; one-pot, single catalyst process) and indirect routes (bio-substrate → isolated intermediate → lactone; multi-pot/multi-catalyst process). Gibbs free energy analysis indicates that oxidative dehydrocyclization of diols to lactones is thermodynamically favourable, whereas non-oxidative diol dehydrocyclization, hydroxy acid esterification, and dicarboxylic acid reduction followed by esterification are generally endergonic. For the indirect route involving dehydration of vicinal diols to epoxides, Gibbs free energy analysis evinces that, while this transformation is usually thermodynamically hindered, diols with longer carbon chains and a higher number of alkyl substituents exhibit more favourable thermodynamics than shorter chain or less-substituted variants to form the epoxide products. The thermodynamic considerations in turn inform critical process design choices including reactor configuration (batch, semi-batch or continuous), phase behaviour (liquid versus vapour), separation strategies, and solvent selection.

In terms of catalyst design principles for the various routes, literature suggests that supported group I oxides can dehydrate vicinal diols to epoxides, which can further be readily carbonylated to β-lactones using homogeneous catalysts or heterogenized variants of the homogeneous catalysts. Redox-active and basic oxides facilitate oxidative dehydrocyclization of non-vicinal diols to lactones, co-producing H_2O. Metal catalysts enable non-oxidative diol dehydrocyclization in the vapour phase under H_2 co-flow, required to keep the metallic sites reduced. Base-poisoned acidic oxides catalyse hydroxy acid esterification, whereas metal-supported acidic oxides hydrogenate and esterify dicarboxylic acids to lactones. Analysis of the biological and biomass-derivable chemo-catalytic pathways to produce these substrates that can then be directly or indirectly converted to lactones indicates that multiple relevant substrates are readily accessible from various metabolic and chemo-catalytic pathways.

The transition to bio-based monomers for circular polymers presents a unique opportunity to reduce dependence on fossil resources and reconfigure supply chains and chemical infrastructure. By leveraging biologically derived feedstocks, novel intermediates with tailored functionality — such as oxygen-rich molecules amenable to lactone and epoxide formation — can be accessed, enabling new materials with enhanced performance and sustainability. However, realizing this potential requires the development of catalytic processes that can efficiently convert these bio-based intermediates into the desired polymerizable lactones. Advances in catalyst design must be driven by a deep mechanistic understanding of selective bond activation, guided by both computational and experimental insights. Furthermore, the integration of past and present knowledge in catalyst and process design is critical for accelerating innovation, ensuring that emerging catalytic strategies align with scalable, industrially viable processes.

Published online: 22 October 2025

References

1. Bachmann, M. et al. Towards circular plastics within planetary boundaries. *Nat. Sustain.* **6**, 599–610 (2023).
2. Zhu, J.-B., Watson, E. M., Tang, J. & Chen, E. Y.-X. A synthetic polymer system with repeatable chemical recyclability. *Science* **360**, 398–403 (2018).
3. Shi, C. et al. Design principles for intrinsically circular polymers with tunable properties. *Chem* **7**, 2896–2912 (2021).
4. Luo, X. et al. Circularly recyclable polymers featuring topochemically weakened carbon–carbon bonds. *J. Am. Chem. Soc.* **144**, 16588–16597 (2022).
5. Helms, B. A. Polydiketoenamines for a circular plastics economy. *Acc. Chem. Res.* **55**, 2753–2765 (2022).
6. Eck, M. & Mecking, S. Closed-loop recyclable and nonpersistent polyethylene-like polyesters. *Acc. Chem. Res.* **57**, 971–980 (2024).
7. Haque, F. M. et al. Defining the macromolecules of tomorrow through synergistic sustainable polymer research. *Chem. Rev.* **122**, 6322–6373 (2022).
8. Zhu, Y., Romain, C. & Williams, C. K. Sustainable polymers from renewable resources. *Nature* **540**, 354–362 (2016).

9. Shi, C., Quinn, E. C., Diment, W. T. & Chen, E. Y. X. Recyclable and (bio)degradable polyesters in a circular plastics economy. *Chem. Rev.* **124**, 4393–4478 (2024).
10. Coates, G. W. & Getzler, Y. D. Y. L. Chemical recycling to monomer for an ideal, circular polymer economy. *Nat. Rev. Mater.* **5**, 501–516 (2020).
11. Ellis, L. D. et al. Chemical and biological catalysis for plastics recycling and upcycling. *Nat. Catal.* **4**, 539–556 (2021).
12. Rahimi, A. & García, J. M. Chemical recycling of waste plastics for new materials production. *Nat. Rev. Chem.* **1**, 0046 (2017).
13. Zhang, Z., Gowda, R. R. & Chen, E. Y. X. Chemosynthetic P4HB: a ten-year journey from a 'non-polymerizable' monomer to a high-performance biomaterial. *Acc. Mater. Res.* **5**, 1340–1352 (2024).
14. Nicholson, S. R., Rorrer, N. A., Carpenter, A. C. & Beckham, G. T. Manufacturing energy and greenhouse gas emissions associated with plastics consumption. *Joule* **5**, 673–686 (2021).
15. Zhou, L. et al. Chemically circular, mechanically tough, and melt-processable polyhydroxyalkanoates. *Science* **380**, 64–69 (2023).
16. Zhou, Z., LaPointe, A. M., Shaffer, T. D. & Coates, G. W. Nature-inspired methylated polyhydroxybutyrates from C1 and C4 feedstocks. *Nat. Chem.* **15**, 856–861 (2023).
17. Kim, M. S. et al. A review of biodegradable plastics: chemistry, applications, properties, and future research needs. *Chem. Rev.* **123**, 9915–9939 (2023).
18. Tang, X. & Chen, E. Y. X. Chemical synthesis of perfectly isotactic and high melting bacterial poly(3-hydroxybutyrate) from bio-sourced racemic cyclic diolide. *Nat. Commun.* **9**, 2345 (2018).
19. Ritz, J., Fuchs, H., Kieczka, H. & Moran, W. C. in *Ullmann's Encyclopedia of Industrial Chemistry* (Wiley, 2000).
20. Jochen, H. et al. Dehydrogenation of 1,4-butanediol to γ-butyrolactone. US patent, 5955620A (1999).
21. Young, F. G. & Fitzpatrick, J. T. β-Hydroxycarboxylic acids and lactones. US patent 2,580,714 (1952).
22. Sixt, J. β-Butyrolactone from diketene. US patent 2,763,664 (1956).
23. Luinstra, G., Molnar, F., Rieger, B. & Allmendinger, M. Catalyst and procedure for the carbonylation of oxiranes. DE10235317 (2004).
24. Stadler, B. M., Wulf, C., Werner, T., Tin, S. & de Vries, J. G. Catalytic approaches to monomers for polymers based on renewables. *ACS Catal.* **9**, 8012–8067 (2019).
25. Huo, J. & Shanks, B. H. Bioprivileged molecules: integrating biological and chemical catalysis for biomass conversion. *Annu. Rev. Chem. Biomol. Eng.* **11**, 63–85 (2020).
26. Kramer, J. W., Lobkovsky, E. B. & Coates, G. W. Practical β-lactone synthesis: epoxide carbonylation at 1 atm. *Org. Lett.* **8**, 3709–3712 (2006).
27. Kramer, J. W., Rowley, J. M. & Coates, G. W. *Organic Reactions* 1–104 (Wiley, 2015).
28. Park, H. D., Dincă, M. & Román-Leshkov, Y. Heterogeneous epoxide carbonylation by cooperative ion-pair catalysis in Co(CO)4^{-}-incorporated Cr-MIL-101. *ACS Cent. Sci.* **3**, 444–448 (2017).
29. Tran, V. G. et al. An end-to-end pipeline for succinic acid production at an industrially relevant scale using *Issatchenkia orientalis*. *Nat. Commun.* **14**, 6152 (2023).
30. Han, T., Kim, G. B. & Lee, S. Y. Glutaric acid production by systems metabolic engineering of an L-lysine-overproducing *Corynebacterium glutamicum*. *Proc. Natl Acad. Sci. USA* **117**, 30328–30334 (2020).
31. Choi, S., Kim, H. U., Kim, T. Y. & Lee, S. Y. Systematic engineering of TCA cycle for optimal production of a four-carbon platform chemical 4-hydroxybutyric acid in *Escherichia coli*. *Metab. Eng.* **38**, 264–273 (2016).
32. Sohn, Y. J. et al. Fermentative high-level production of 5-hydroxyvaleric acid by metabolically engineered *Corynebacterium glutamicum*. *ACS Sustain. Chem. Eng.* **9**, 2523–2533 (2021).
33. Ewell, R. H. & Eyring, H. Theory of the viscosity of liquids as a function of temperature and pressure. *J. Chem. Phys.* **5**, 726–736 (1937).
34. Chen, S.-C., Hsu, L.-A., Lin, F.-S. & Tsai, C.-L. Method for preparing lactone. European Patent EP1214972A1 (2000).
35. Touchy, A. S. & Shimizu, K.-I. Acceptorless dehydrogenative lactonization of diols by Pt-loaded SnO_2 catalysts. *RSC Adv.* **5**, 29072–29075 (2015).
36. Zhong, W., Liu, H., Bai, C., Liao, S. & Li, Y. Base-free oxidation of alcohols to esters at room temperature and atmospheric conditions using nanoscale co-based catalysts. *ACS Catal.* **5**, 1850–1856 (2015).
37. Eagan, N. M., Kumbhalkar, M. D., Buchanan, J. S., Dumesic, J. A. & Huber, G. W. Chemistries and processes for the conversion of ethanol into middle-distillate fuels. *Nat. Rev. Chem.* **3**, 223–249 (2019).
38. Kim, T. Y. et al. Gas-phase dehydration of vicinal diols to epoxides: dehydrative epoxidation over a Cs/SiO_2 catalyst. *J. Catal.* **323**, 85–99 (2015).
39. Kostal, J. & Jorgensen, W. L. Thorpe–Ingold acceleration of oxirane formation is mostly a solvent effect. *J. Am. Chem. Soc.* **132**, 8766–8773 (2010).
40. Zhou, L. et al. Chain-end controlled depolymerization selectivity in α,α-disubstituted propionate PHAs with dual closed-loop recycling and record-high melting temperature. *J. Am. Chem. Soc.* **146**, 29895–29904 (2024).
41. Badlani, M. & Wachs, I. E. Methanol: a 'smart' chemical probe molecule. *Catal. Lett.* **75**, 137–149 (2001).
42. Duan, H., Yamada, Y., Kubo, S. & Sato, S. Vapor-phase catalytic dehydration of 2,3-butanediol to 3-buten-2-ol over ZrO_2 modified with alkaline earth metal oxides. *Appl. Catal. A Gen.* **530**, 66–74 (2017).
43. Burcham, L. J., Badlani, M. & Wachs, I. E. The origin of the ligand effect in metal oxide catalysts: novel fixed-bed in situ infrared and kinetic studies during methanol oxidation. *J. Catal.* **203**, 104–121 (2001).
44. Zhang, B., Ford, M. E., Ream, E. & Wachs, I. E. Olefin metathesis over supported MoO_x catalysts: influence of the oxide support. *Catal. Sci. Technol.* **13**, 217–225 (2023).
45. Kiani, D. & Baltrusaitis, J. A spectroscopic study of supported-phosphate-catalysts (SPCs): evidence of surface-mediated hydrogen-transfer. *ChemCatChem* **13**, 2064–2073 (2021).
46. Zhang, W., Yu, D., Ji, X. & Huang, H. Efficient dehydration of bio-based 2,3-butanediol to butanone over boric acid modified HZSM-5 zeolites. *Green Chem.* **14**, 3441–3450 (2012).
47. Ramayya, S., Brittain, A., DeAlmeida, C., Mok, W. & Antal, M. J. Acid-catalysed dehydration of alcohols in supercritical water. *Fuel* **66**, 1364–1371 (1987).
48. Jung, M. E. & Piizzi, G. Gem-disubstituent effect: theoretical basis and synthetic applications. *Chem. Rev.* **105**, 1735–1766 (2005).
49. Grant, J. T., Carrero, C. A., Love, A. M., Verel, R. & Hermans, I. Enhanced two-dimensional dispersion of group V metal oxides on silica. *ACS Catal.* **5**, 5787–5793 (2015).
50. Kiani, D., Sourav, S., Wachs, I. E. & Baltrusaitis, J. Synthesis and molecular structure of model silica-supported tungsten oxide catalysts for oxidative coupling of methane (OCM). *Catal. Sci. Technol.* **10**, 3334–3345 (2020).
51. Kiani, D. et al. Existence and properties of isolated catalytic sites on the surface of β-cristobalite-supported, doped tungsten oxide catalysts (WO_x/β-SiO_2, Na-WO_x/β-SiO_2, Mn-WO_x/β-SiO_2) for oxidative coupling of methane (OCM): a combined periodic DFT and experimental study. *ACS Catal.* **10**, 4580–4592 (2020).
52. Hou, S., Cao, Y., Xiong, W., Liu, H. & Kou, Y. Site requirements for the oxidative coupling of methane on SiO_2-supported Mn catalysts. *Ind. Eng. Chem. Res.* **45**, 7077–7083 (2006).
53. Kiani, D., Sourav, S., Baltrusaitis, J. & Wachs, I. E. Oxidative coupling of methane (OCM) by SiO_2-supported tungsten oxide catalysts promoted with Mn and Na. *ACS Catal.* **9**, 5912–5928 (2019).
54. Jiang, J. & Yoon, S. A metalated porous porphyrin polymer with $[Co(CO)_4]^-$ anion as an efficient heterogeneous catalyst for ring expanding carbonylation. *Sci. Rep.* **8**, 13243 (2018).
55. Rajendiran, S., Natarajan, P. & Yoon, S. A covalent triazine framework-based heterogenized Al–Co bimetallic catalyst for the ring-expansion carbonylation of epoxide to β-lactone. *RSC Adv.* **7**, 4635–4638 (2017).
56. Park, H. D., Dincă, M. & Román-Leshkov, Y. Continuous-flow production of succinic anhydrides via catalytic β-lactone carbonylation by $Co(CO)_4$⊂Cr-MIL-101. *J. Am. Chem. Soc.* **140**, 10669–10672 (2018).
57. Ichikawa, N., Sato, S., Takahashi, R., Sodesawa, T. & Inui, K. Dehydrogenative cyclization of 1,4-butanediol over copper-based catalyst. *J. Mol. Catal. A Chem.* **212**, 197–203 (2004).
58. Nagaiah, P. et al. Selective vapour phase dehydrogenation of biomass-derived 1,4-butanediol to gamma butyrolactone over Cu/ZrO_2 catalysts: influence of La_2O_3 promotor. *Res. Chem. Intermed.* **44**, 5817–5831 (2018).
59. Chong, S. et al. Enhanced the dehydrocyclization of 1,4-butanediol to γ-butyrolactone via the regulation of interface oxygen vacancies in Cu/MgO-CeO_2 catalyst. *Chem. Eng. J.* **489**, 151366 (2024).
60. Huang, J., Wang, Y., Zheng, J., Dai, W.-L. & Fan, K. Influence of support surface basicity and gold particle size on catalytic activity of Au/γ-AlOOH and Au/γ-Al_2O_3 catalyst in aerobic oxidation of α,ω-diols to lactones. *Appl. Catal. B Environ.* **103**, 343–350 (2011).
61. Huang, J., Dai, W.-L., Li, H. & Fan, K. Au/TiO_2 as high efficient catalyst for the selective oxidative cyclization of 1,4-butanediol to γ-butyrolactone. *J. Catal.* **252**, 69–76 (2007).
62. Jarvis, J. S. et al. Inhibiting the dealkylation of basic arenes during *n*-alkane direct aromatization reactions and understanding the C6 ring closure mechanism. *ACS Catal.* **10**, 8428–8443 (2020).
63. Miller, J. T., Agrawal, N. G. B., Lane, G. S. & Modica, F. S. Effect of pore geometry on ring closure selectivities in platinum L-zeolite dehydrocyclization catalysts. *J. Catal.* **163**, 106–116 (1996).
64. Huang, J., Dai, W.-L. & Fan, K. Support effect of new Au/FeO_x catalysts in the oxidative dehydrogenation of α,ω-diols to lactones. *J. Phys. Chem. C* **112**, 16110–16117 (2008).
65. Chen, A. et al. Structure of the catalytically active copper–ceria interfacial perimeter. *Nat. Catal.* **2**, 334–341 (2019).
66. Li, X. et al. Ethanol dehydrogenation to acetaldehyde over a $Cu^{\delta+}$-based Cu-MFI catalyst. *Chin. J. Catal.* **49**, 91–101 (2023).
67. Hanukovich, S., Dang, A. & Christopher, P. Influence of metal oxide support acid sites on Cu-catalyzed nonoxidative dehydrogenation of ethanol to acetaldehyde. *ACS Catal.* **9**, 3537–3550 (2019).
68. Wang, C. et al. Low-temperature dehydrogenation of ethanol on atomically dispersed gold supported on $ZnZrO_x$. *ACS Catal.* **6**, 210–218 (2016).
69. Farnesi Camellone, M. & Marx, D. Nature and role of activated molecular oxygen species at the gold/titania interface in the selective oxidation of alcohols. *J. Phys. Chem. C* **118**, 20989–21000 (2014).
70. Yi, N., Si, R., Saltsburg, H. & Flytzani-Stephanopoulos, M. Active gold species on cerium oxide nanoshapes for methanol steam reforming and the water gas shift reactions. *Energy Environ. Sci.* **3**, 831–837 (2010).
71. Wang, T. et al. Nature of metal–support interaction for metal catalysts on oxide supports. *Science* **386**, 915–920 (2024).
72. Wu, P. et al. Harnessing strong metal–support interactions via a reverse route. *Nat. Commun.* **11**, 3042 (2020).
73. van Deelen, T. W., Hernández Mejía, C. & de Jong, K. P. Control of metal–support interactions in heterogeneous catalysts to enhance activity and selectivity. *Nat. Catal.* **2**, 955–970 (2019).

74. Xie, J. et al. Deactivation of supported Pt catalysts during alcohol oxidation elucidated by spectroscopic and kinetic analyses. *ACS Catal.* **7**, 6745–6756 (2017).
75. Wei, Z., Karim, A., Li, Y. & Wang, Y. Elucidation of the roles of re in aqueous-phase reforming of glycerol over Pt–Re/C Catalysts. *ACS Catal.* **5**, 7312–7320 (2015).
76. Galley, R. Processes for the manufacture of lactones. WO2002016346 (2002).
77. Wu, X., Guo, J., Lv, W. & Jia, Z. Green preparation of four-membered ring beta-lactones. CN116283840 (2023).
78. Whittingham, M. S. Solid-state ionics: the key to the discovery and domination of lithium batteries: some learnings from β-alumina and titanium disulfide. *MRS Bull.* **46**, 168–173 (2021).
79. You, C., Zhang, C., Chen, L. & Qi, Z. Highly dispersed palladium nanoclusters incorporated in amino-functionalized silica spheres for the selective hydrogenation of succinic acid to γ-butyrolactone. *Appl. Organomet. Chem.* **29**, 653–660 (2015).
80. Le, S. D. & Nishimura, S. Highly selective synthesis of 1,4-butanediol via hydrogenation of succinic acid with supported Cu–Pd alloy nanoparticles. *ACS Sustain. Chem. Eng.* **7**, 18483–18492 (2019).
81. Tapin, B. et al. Study of monometallic Pd/TiO_2 catalysts for the hydrogenation of succinic acid in aqueous phase. *ACS Catal.* **3**, 2327–2335 (2013).
82. Zhang, C., Chen, L., Cheng, H., Zhu, X. & Qi, Z. Atomically dispersed Pd catalysts for the selective hydrogenation of succinic acid to γ-butyrolactone. *Catal. Today* **276**, 55–61 (2016).
83. Heisig, C., Diedenhoven, J., Jensen, C., Gehrke, H. & Turek, T. Selective hydrogenation of biomass-derived succinic acid: reaction network and kinetics. *Chem. Eng. Technol.* **43**, 484–492 (2020).
84. Hayes, G. et al. Polymers without petrochemicals: sustainable routes to conventional monomers. *Chem. Rev.* **123**, 2609–2734 (2023).
85. Abou Hamdan, M., Loridant, S., Jahjah, M., Pinel, C. & Perret, N. TiO_2-supported molybdenum carbide: an active catalyst for the aqueous phase hydrogenation of succinic acid. *Appl. Catal. A Gen.* **571**, 71–81 (2019).
86. Hamdan, M. A. et al. Influence of reduction–carburization parameters on the performance of supported molybdenum carbide catalysts in succinic acid hydrogenation. *Ind. Eng. Chem. Res.* **59**, 12964–12976 (2020).
87. Khusnutdinov, R. I., Shchadneva, N. A., Baiguzina, A. R., Lavrentieva, Y. Y. & Dzhemilev, U. M. Generation of alkyl hypochlorites in oxidation of alcohols with carbon tetrachloride catalyzed by vanadium and manganese compounds. *Russ. Chem. Bull.* **51**, 2074–2079 (2002).
88. Bhatia, A., Kannan, M. & Muthaiah, S. Ruthenium-promoted acceptorless and oxidant-free lactone synthesis in aqueous medium. *Synlett* **30**, 721–725 (2019).
89. Tanzawa, T. & Schwartz, J. Catalytic conversion of beta-hydroxy carboxylic acids to olefins by tungsten(VI) complexes: a new acyl group transfer catalyst. *Organometallics* **9**, 3026–3027 (1990).
90. Zhuang, Z. & Yu, J.-Q. Lactonization as a general route to β-C(sp^3)–H functionalization. *Nature* **577**, 656–659 (2020).
91. Molnar, F., Luinstra, G. A., Allmendinger, M. & Rieger, B. Multisite catalysis: a mechanistic study of β-lactone synthesis from epoxides and CO — insights into a difficult case of homogeneous catalysis. *Chem. Eur. J.* **9**, 1273–1280 (2003).
92. Church, T. L., Getzler, Y. D. Y. L. & Coates, G. W. The mechanism of epoxide carbonylation by [Lewis acid]+[$Co(CO)_4$]$^-$ catalysts. *J. Am. Chem. Soc.* **128**, 10125–10133 (2006).
93. Schmidt, J. A. R., Lobkovsky, E. B. & Coates, G. W. Chromium(III) octaethylporphyrinato tetracarbonylcobaltate: a highly active, selective, and versatile catalyst for epoxide carbonylation. *J. Am. Chem. Soc.* **127**, 11426–11435 (2005).
94. Schmidt, J. A. R., Mahadevan, V., Getzler, Y. D. Y. L. & Coates, G. W. A readily synthesized and highly active epoxide carbonylation catalyst based on a chromium porphyrin framework: expanding the range of available β-lactones. *Org. Lett.* **6**, 373–376 (2004).
95. Mahadevan, V., Getzler, Y. D. Y. L. & Coates, G. W. [Lewis acid]+[$Co(CO)_4$]$^-$ complexes: a versatile class of catalysts for carbonylative ring expansion of epoxides and aziridines. *Angew. Chem. Int. Ed.* **41**, 2781–2784 (2002).
96. Getzler, Y. D. Y. L., Mahadevan, V., Lobkovsky, E. B. & Coates, G. W. Synthesis of β-lactones: a highly active and selective catalyst for epoxide carbonylation. *J. Am. Chem. Soc.* **124**, 1174–1175 (2002).
97. Rowley, J. M., Lobkovsky, E. B. & Coates, G. W. Catalytic double carbonylation of epoxides to succinic anhydrides: catalyst discovery, reaction scope, and mechanism. *J. Am. Chem. Soc.* **129**, 4948–4960 (2007).
98. Linger, J. G. et al. Lignin valorization through integrated biological funneling and chemical catalysis. *Proc. Natl Acad. Sci. USA* **111**, 12013–12018 (2014).
99. Pitzalis, M. F. & Sadler, J. C. Chemical bio-manufacture from diverse C-rich waste polymeric feedstocks using engineered microorganisms. *RSC Sustain.* **3**, 1672–1684 (2025).
100. Sullivan, K. P. et al. Mixed plastics waste valorization through tandem chemical oxidation and biological funneling. *Science* **378**, 207–211 (2022).
101. Wu, X., De Bruyn, M. & Barta, K. Deriving high value products from depolymerized lignin oil, aided by (bio)catalytic funneling strategies. *Chem. Commun.* **59**, 9929–9951 (2023).
102. Delidovich, I. et al. Alternative monomers based on lignocellulose and their use for polymer production. *Chem. Rev.* **116**, 1540–1599 (2016).
103. Cen, X., Dong, Y., Liu, D. & Chen, Z. New pathways and metabolic engineering strategies for microbial synthesis of diols. *Curr. Opin. Biotechnol.* **78**, 102845 (2022).
104. Lee, S. Y. et al. A comprehensive metabolic map for production of bio-based chemicals. *Nat. Catal.* **2**, 18–33 (2019).
105. Jang, W. D., Kim, G. B. & Lee, S. Y. An interactive metabolic map of bio-based chemicals. *Trends Biotechnol.* **41**, 10–14 (2023).
106. Giarola, S., Romain, C., Williams, C. K., Hallett, J. P. & Shah, N. in *Computer Aided Chemical Engineering* Vol. 37 (eds Krist, V. G. et al.) 2561–2566 (Elsevier, 2015).
107. Zhang, L. et al. Highly selective hydrogenation of phthalic anhydride to phthalide over $CoSi_x$/CNTs catalyst prepared by multi-step microwave-assisted chemical vapor deposition. *Mater. Chem. Phys.* **180**, 89–96 (2016).
108. Mahmoud, E., Watson, D. A. & Lobo, R. F. Renewable production of phthalic anhydride from biomass-derived furan and maleic anhydride. *Green Chem.* **16**, 167–175 (2014).
109. Yuan, L. et al. Production of copolyester monomers from plant-based acrylate and acetaldehyde. *Angew. Chem. Int. Ed.* **61**, e202113471 (2022).
110. Hu, Y. et al. Synthesis of 1,4-cyclohexanedimethanol, 1,4-cyclohexanedicarboxylic acid and 1,2-cyclohexanedicarboxylates from formaldehyde, crotonaldehyde and acrylate/fumarate. *Angew. Chem. Int. Ed.* **57**, 6901–6905 (2018).
111. Chokhawala, H. A high yield route for the production of compounds from renewable sources. Europe patent 3047030A2 (2014).
112. He, J. et al. Synthesis of 1,6-hexanediol from cellulose derived tetrahydrofuran-dimethanol with Pt-WO_x/TiO_2 catalysts. *ACS Catal.* **8**, 1427–1439 (2018).
113. Buntara, T. et al. Caprolactam from renewable resources: catalytic conversion of 5-hydroxymethylfurfural into caprolactone. *Angew. Chem. Int. Ed.* **50**, 7083–7087 (2011).
114. Burt, S. P. et al. Production of 1,6-hexanediol from tetrahydropyran-2-methanol by dehydration–hydration and hydrogenation. *Green Chem.* **19**, 1390–1398 (2017).
115. Liu, Y., Cen, X., Liu, D. & Chen, Z. Metabolic engineering of *Escherichia coli* for high-yield production of (R)-1,3-butanediol. *ACS Synth. Biol.* **10**, 1946–1955 (2021).
116. Islam, T., Nguyen-Vo, T. P., Gaur, V. K., Lee, J. & Park, S. Metabolic engineering of *Escherichia coli* for biological production of 1, 3-butanediol. *Bioresour. Technol.* **376**, 128911 (2023).
117. Barton, N. R. et al. An integrated biotechnology platform for developing sustainable chemical processes. *J. Ind. Microbiol. Biotechnol.* **42**, 349–360 (2015).
118. Cargill to build biobased 1,4-butanediol plant. *C&EN Global Enterprise* https://doi.org/10.1021/cen-09922-buscon2 (2021).
119. GENOMATICA TO GO PUBLIC. *Chemical & Engineering News Archive* https://doi.org/10.1021/cen-v089n035.p008a (2011).
120. Rohles, C. M. et al. A bio-based route to the carbon-5 chemical glutaric acid and to bionylon-6,5 using metabolically engineered *Corynebacterium glutamicum*. *Green Chem.* **20**, 4662–4674 (2018).
121. Huang, K. et al. Conversion of furfural to 1,5-pentanediol: process synthesis and analysis. *ACS Sustain. Chem. Eng.* **5**, 4699–4706 (2017).
122. Brentzel, Z. J. et al. Chemicals from biomass: combining ring-opening tautomerization and hydrogenation reactions to produce 1,5-pentanediol from furfural. *ChemSusChem* **10**, 1351–1355 (2017).
123. Dastidar, R. G. et al. Catalytic production of δ-valerolactone (DVL) from biobased 2-hydroxytetrahydropyran (HTHP) — combined experimental and modeling study. *Appl. Catal. B Environ. Energy* **360**, 124519 (2025).

Acknowledgements

Funding was provided by the US Department of Energy, Office of Energy Efficiency and Renewable Energy, Advanced Materials and Manufacturing Office (AMMTO) and Bioenergy Technologies Office (BETO). This work was performed as part of the Bio-Optimized Technologies to keep Thermoplastics out of Landfills and the Environment (BOTTLE) Consortium and was supported by AMMTO and BETO at the National Renewable Energy Laboratory for the US Department of Energy (DOE) under Contract No. DE-AC36-08GO28308. The BOTTLE Consortium includes members from Massachusetts Institute of Technology, University of Puerto Rico — Mayagüez, and Colorado State University. D.K. was in part supported by the Director's Fellowship — Laboratory Directed Research and Development (LDRD) Program at NREL. The views expressed in the article do not necessarily represent the views of the DOE or the US Government. The US Government retains and the publisher, by accepting the article for publication, acknowledges that the US Government retains a non-exclusive, paid-up, irrevocable, worldwide licence to publish or reproduce the published form of this work, or allow others to do so, for US Government purposes. The authors thank S. Mohammed for help with the Gibbs free energy analysis.

Author contributions

G.T.B. and D.K. conceptualized the review. D.K. was responsible for data curation. G.T.B., D.K., R.E., J.H.M. and A.Z.W. were responsible for formal analysis and visualization. All authors were involved in writing, reviewing, and editing drafts of the manuscript. G.T.B. supervised and administered the project and was responsible for funding acquisition.

Competing interests

Several of the authors have filed patent applications on chemo-catalytic lactone production, but the specific technology is not discussed herein. D.K. and G.T.B. are inventors on a patent application (US patent application no. 63/790,923) that covers lactone production from diols. J.H.M., E.Y.-X.C., and G.T.B. are inventors on a patent application (US patent application no. 63/843,527) that covers β-lactone production. Y.R.-L. is an inventor on a patent application (US patent application no. 19/279,265) that covers a continuous method for producing lactones.

Additional information

Supplementary information The online version contains supplementary material available at https://doi.org/10.1038/s41570-025-00765-9.

Peer review information *Nature Reviews Chemistry* thanks Mukund Sibi, George Huber, and the other, anonymous, reviewer(s) for their contribution to the peer review of this work.